

May 2015

# Paleoredox Geochemistry and Bioturbation Levels of the Exceptionally Preserved Early Cambrian Indian Springs Biota, Poleta Formation, Nevada, USA

Jonah Meron Novek  
*University of Wisconsin-Milwaukee*

Follow this and additional works at: <https://dc.uwm.edu/etd>

 Part of the [Ecology and Evolutionary Biology Commons](#), [Geochemistry Commons](#), and the [Geology Commons](#)

---

## Recommended Citation

Novek, Jonah Meron, "Paleoredox Geochemistry and Bioturbation Levels of the Exceptionally Preserved Early Cambrian Indian Springs Biota, Poleta Formation, Nevada, USA" (2015). *Theses and Dissertations*. 826.  
<https://dc.uwm.edu/etd/826>

This Thesis is brought to you for free and open access by UWM Digital Commons. It has been accepted for inclusion in Theses and Dissertations by an authorized administrator of UWM Digital Commons. For more information, please contact [open-access@uwm.edu](mailto:open-access@uwm.edu).

PALEOREDOX GEOCHEMISTRY AND BIOTURBATION LEVELS OF THE  
EXCEPTIONALLY PRESERVED EARLY CAMBRIAN INDIAN SPRINGS BIOTA,  
POLETA FORMATION, NEVADA, USA

by

Jonah M. Novek

A Thesis Submitted in  
Partial Fulfillment of the  
Requirements for the Degree of

Master of Science  
in Geosciences

at

The University of Wisconsin-Milwaukee

May 2015

ABSTRACT  
PALEOREDOX GEOCHEMISTRY AND BIOTURBATION LEVELS OF THE  
EXCEPTIONALLY PRESERVED EARLY CAMBRIAN INDIAN SPRINGS BIOTA,  
POLETA FORMATION, NEVADA, USA

by

Jonah M. Novek

The University of Wisconsin-Milwaukee, 2015  
Under the Supervision of Professor Stephen Q. Dornbos

The early Cambrian Indian Springs biota, western Nevada, USA exhibits Burgess Shale-type (BST) preservation of a diverse array of animal phyla, including the earliest definitive echinoderms. It therefore provides an important window on animal life during the Cambrian radiation. The objective of this study is to analyze the trace metal paleoredox geochemistry and bioturbation levels of this BST deposit in order to characterize the paleoenvironmental conditions in which these animals lived and their fossils were preserved. A total of 28 rock samples were collected from outcrops at three previously reported intervals of exceptional preservation at the Indian Springs locality, as well as at one interval not known to exhibit such preservation. An additional 20 random samples were collected from the talus for comparison. In the laboratory, the samples were geochemically analyzed for trace metal paleoredox indices (V/Cr and V/(V+Ni) ratios) and bioturbation levels were assessed through X-radiography and petrographic thin sections using the ichnofabric index (ii) method. Additional samples from coeval strata of the Poleta Formation in the White-Inyo Mountains, CA that lack BST preservation were also geochemically analyzed with the same methodology. Preliminary results indicate that oxic bottom water conditions dominated during deposition of these strata, despite consistently low bioturbation levels. This pattern holds for intervals with BST preservation and those

without. Although ephemeral incursions of low-oxygen waters may have taken place, there is no evidence for persistent oxygen restriction in these paleoenvironments. The low levels of bioturbation indicate limited mixed layer development and a redox boundary near the sediment-water interface, likely allowing post-burial BST preservation to occur even in this setting dominated by oxic bottom waters. Paleoecological reconstructions and taphonomic hypotheses relating to the Indian Springs Lagerstätte should account for the paleoredox conditions revealed in this study. Several models propose the roles of clay minerals, the presence of hypersaline brines, and the actions of Fe-reducing bacteria as mechanisms for exceptional preservation.

© Copyright by Jonah Novek, 2015  
All Rights Reserved

## TABLE OF CONTENTS

List of Figures.....	vi
Acknowledgements.....	viii
1. Introduction.....	1
2. Previous work.....	3
2.1 Cambrian substrate revolution.....	3
2.2 Paleoredox geochemistry of Burgess Shale-type deposits.....	4
2.3 The Indian Springs biota and correlative strata.....	8
3. Geologic setting.....	11
4. Methods.....	14
4.1 Field methods.....	14
4.2 Laboratory methods.....	15
5. Results.....	18
5.1 Paleoredox geochemistry.....	18
5.2 Bioturbation levels and microfacies.....	25
6. Discussion.....	28
7. Conclusions.....	30
References.....	32
Appendix A: Photos of Field Location at Indian Springs Canyon, NV.....	37
Appendix B: Table of Detailed Locality Information .....	46
Appendix C: X-radiograph Images .....	48
Appendix D: Thin Sections From ISP1 and ISP2 (in Plane Polar Light).....	51
Appendix E: XRF Geochemical Data X-radiograph Images.....	65
Appendix F: Ichnofabric Index Data and Measurements .....	83

## LIST OF FIGURES

Figure	Page
1. Locality map. A. Eastern California and western Nevada. B. Location of Indian Springs Canyon (N37° 43.488, W 117° 19.186), Esmeralda County, western Nevada and Westgard Pass ( <b>GPS</b> ), White-Inyo Mountains, eastern California (after English and Babcock, 2010). C. Regional lower Cambrian stratigraphic column. Arrow indicates the Middle Member of the Poleta formation.....	2
2. Strat column (in meters) of Indian Springs locality showing base of the middle member of the Poleta Formation. Arrows indicate sampling intervals.....	9
3. Paleogeographic map of North America during the early Cambrian. From <a href="http://jan.ucc.nau.edu/~rcb7/namC510.jpg">http://jan.ucc.nau.edu/~rcb7/namC510.jpg</a> .....	12
4. Chart displaying five paleoredox indices identified by Jones and Manning (1994) as most reliable. V/Cr is utilized for this study .....	16
5. Paleoredox indices (V/Cr and V/(V+Ni)), ichnofabric indices, and microstratigraphy (event beds vs. background sedimentation) of 20 m horizon (ISP1) at Indian Springs. Event beds are dotted intervals (graded beds). Background sedimentation shown as thin lines (laminations).....	20
6. Paleoredox indices (V/Cr and V/(V+Ni)), ichnofabric indices, and microstratigraphy (event beds vs. background sedimentation) of 65 m horizon (ISP2) at Indian Springs. Event beds are dotted intervals (graded beds). Background sedimentation shown as thin lines (laminations).....	21
7. Paleoredox indices (V/Cr and V/(V+Ni)), ichnofabric indices, and microstratigraphy (event beds vs. background sedimentation) of section from middle member of Poleta Formation at Westgard Pass, White-Inyo Mountains, CA. Samples from Dornbos and Bottjer (2000). Event beds are dotted intervals (graded beds). Background sedimentation shown as thin lines (laminations).....	23
8. V/Cr vs. V/(V+Ni) for the Poleta Formation at Indian Springs and White-Inyo Mountains. Data from Spence Shale, Wheeler Shale, and Maotianshan Shales from Kloss et al. (in review).....	24

9. Thin sections of rock from Indian Springs Canyon. In plain polar light. A. ISP1-2, B. ISP1-4, C. ISP2-3, D. ISP24.....	26
10. X-radiographed slabs of rock samples from ISP1. A. Sample ISP1-6, yellow arrow indicating event bed, red arrow indicating bioturbation in the form of burrows. B. Red arrows indicating background laminations.....	27

## ACKNOWLEDGMENTS

I would like to, first and foremost, thank my advisor, Dr. Stephen Q. Dornbos, for his push, patience, and dedication in guiding me through this thesis. If it were not for him, this project would not have been possible. I would like to thank Dr. Lindsay McHenry and Dr. John Isbell for their support and involvement in this project and their willingness to answer my many questions. I would also like to thank Adam Potts for his relentless field assistance and “good sport” attitude through not always ideal times and conditions.

I would like to thank the following for funding for this project: UWM Department of Geosciences, Wisconsin Geological Society, The Geological Society of America, and the NASA Wisconsin Space Grant Consortium. Without their financial support, this project would not have been possible.

I would also like to thank my family and friends from near and far for their relentless support and push in me to pursue my dreams and desires, no matter where they took me. Lastly, I would like to thank the entire UWM Geoscience department and especially my office mates, Nick Fedorchuk, Nicole Braun, Kit Carson, and Jenny Ulbricht. Were it not for their undying laughter, advice, good nature, and motivation, I would have not made it through this journey.

## **1. Introduction**

The early Cambrian was a unique time in the history of life on Earth. The Ediacaran-Cambrian transition had dramatic evolutionary and ecological implications resulting in new animal body plans and life modes, an occurrence known as the Cambrian explosion (e.g., Gould, 1989; Babcock, 2005). As new life modes flourished in the early Cambrian, irreversible repercussions on the geochemistry and physical makeup of sediment substrates took place. The increase in animal mixing of sediment, or vertically oriented bioturbation by sediment-dwelling, infaunal, macro-invertebrate organisms (Ciarelli, et al., 1999), led to the first appearance of the mixed layer. This transition in bioturbation depth and intensity is often referred to as the Agronomic Revolution (Seilacher and Pflüger, 1994) and its impact on the evolutionary paleoecology of benthic organisms is referred to as the Cambrian Substrate Revolution (CSR) (Bottjer et al., 2000).

Studying and interpreting deposits with exceptional Burgess Shale-type (BST) preservation greatly enhances understanding of the Cambrian explosion and the CSR. These BST deposits preserve evidence of nonbiomineralized body parts (i.e. soft parts) as carbonaceous compressions in fine-grained marine siliciclastic rocks and show a more complete record of ancient life compared to “normal” fossil deposits that contain only hard parts. The primary focus of this study is the BST deposit known as the Indian Springs biota, which is preserved in the early Cambrian Poleta Formation of the Montezuma Range, western Nevada, USA (Fig. 1) and how ancient oxygen conditions, among other factors, may have led to the exceptional preservation observed..

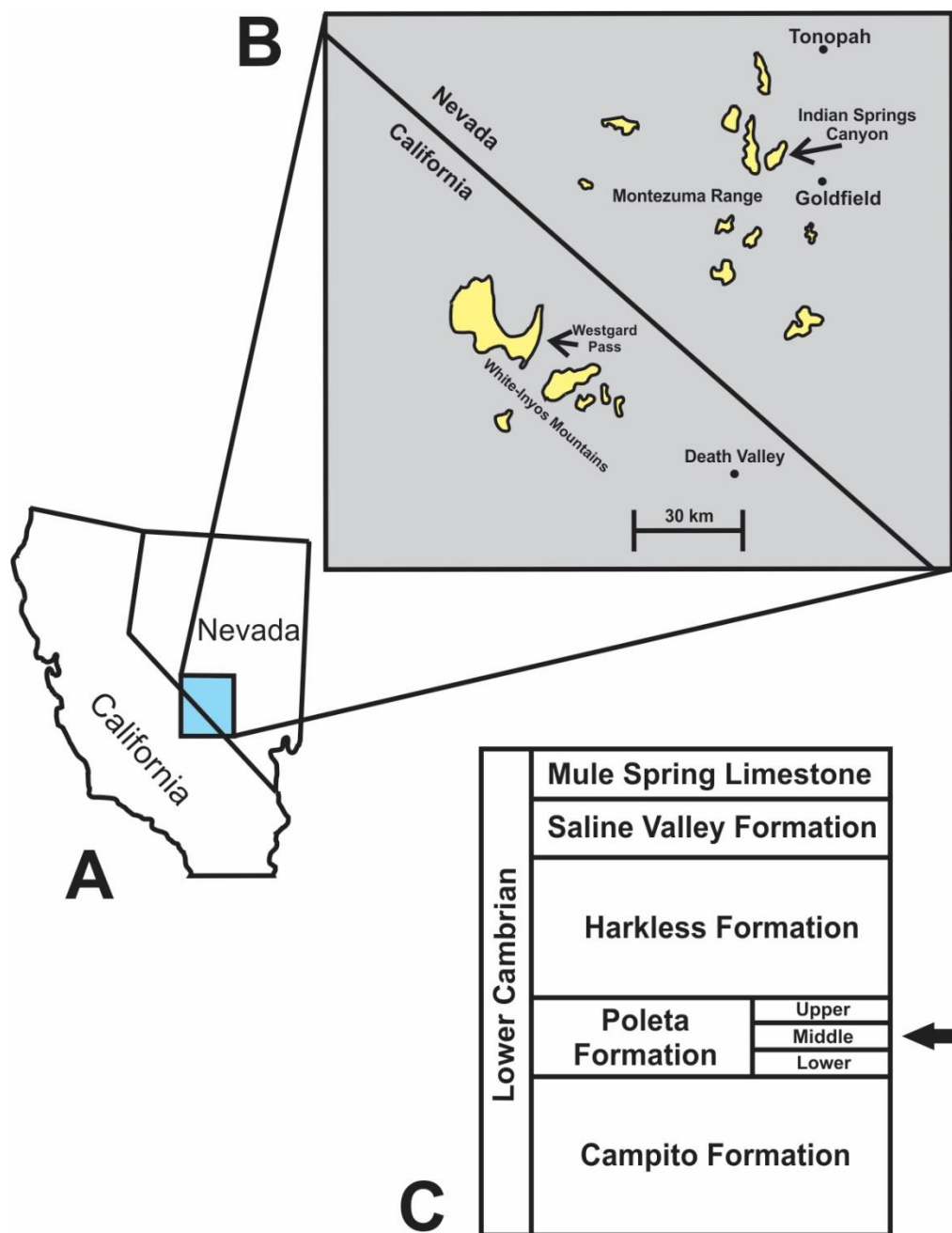


Figure 1 - Locality map. A. Eastern California and western Nevada. B. Location of Indian Springs Canyon (N37° 43.488, W 117° 19.186), Esmeralda County, western Nevada and Westgard Pass (GPS), White-Inyo Mountains, eastern California (after English and Babcock, 2010). C. Regional lower Cambrian stratigraphic column. Arrow indicates the middle member of the Poleta formation.

There are approximately thirty different BST deposits identified and studied globally (e.g. Hagadorn, 2002). Based largely on bioturbation levels, the paleoenvironments for most of these deposits, including the famous Burgess Shale biota, have classically been interpreted as low-oxygen or anoxic (e.g. Landing, 2001; Gaines and Droser, 2003; Garson, et al., 2012). The goal of this study is to test this oxygen restricted hypothesis for BST preservation through reconstructing the bottom water paleoredox conditions of the Indian Springs biota paleoenvironment using trace metal geochemistry and comparing these results with mm-scale bioturbation levels.

## **2. Previous work**

### *2.1 Cambrian substrate revolution*

Late Neoproterozoic to early Phanerozoic marine substrates display a transition from microbial mat-dominated (e.g. Gehling, 1986, 1996, Schieber, 1986, Hagadorn and Bottjer, 1997), water-poor seafloors with minimal vertical bioturbation (e.g. Droser et al., 1999) to substrates dominated by an infauna and subsequent increased levels of vertical bioturbation. As a result, cohesive seafloor microbial mats become increasingly scarce and the Proterozoic-style sharp water-sediment interface became less well defined (Bottjer et al., 2000). The evolutionary and paleoecological implications of this new reworking of horizontal sediment horizons for benthic organisms is referred to as the Cambrian Substrate Revolution (CSR) (Bottjer et al., 2000).

The onset of widespread microphagous, feeding on relatively large particulate matter, predation in the early Cambrian is thought to be one of the driving factors in the evolution of new metazoan morphologies and body plans including biomineralized

skeletons (Vermeij, 1989; Bengtson, 1994). In addition to the appearance and increase in vertical bioturbation in Cambrian substrates, horizontal trace fossils, such as *Plagiogmus* and *Taphrhelminthopsis*, diversified as part of the Cambrian explosion (McIlroy and Heys, 1997; Hagadorn et al., 2000a). Many of these ichnogenera are found in deeper marine deposits after the Cambrian, indicative of an onshore-offshore retreat. This is often seen when a dominant morphology or life mode of organisms forces older organisms to deeper marine facies (Bottjer et al., 1988; Crimes and Fedonkin, 1994). The physical and geochemical changes brought upon these shallow marine environments led to the same type of soft-sediment substrates we commonly observe today in shallow siliciclastic and carbonate marine environments (Bottjer et al., 2000).

## *2.2 Paleoredox geochemistry of Burgess Shale-type deposits*

Multiple paleoredox studies (e.g. Landing, 2001; Gaines and Droser, 2003; Garson et al., 2012) have been conducted on BST deposits largely focusing on trace fossil proxies and seldom analyzing the paleoredox geochemistry of the paleoenvironment. These studies assumed a relationship between low bioturbation levels and dysoxic or anoxic waters, thereby dismissing the possibility that deposits with low bioturbation levels could have been preserved under oxic bottom water conditions. A growing body of geochemical studies, however, calls into question this correlation between low bioturbation levels and oxygen-restricted bottom water conditions in Cambrian BST deposits (Powell et al., 2003, Powell, 2009, McKirdy et al., 2011, Kloss et al., in review).

The geochemical study of marine redox conditions tracks the relative distribution of oxidizing agents across depositional and diagenetic gradients and attempts to understand

the biogeochemical factors that control these processes (Tribovillard et al., 2006). Trace element concentrations in a sample may be used to reconstruct paleoenvironmental conditions depending on whether or not they are relatively enriched or depleted. Often, the degree and amount of enrichment or depletion of trace elements in a sample is evaluated relative to its concentration in average crustal rocks or shales (Wedepohl, 1971, 1991; McLennan, 2001). Organic rich, siliciclastic black and gray shales are often the focus of trace elemental paleoenvironmental work.

Numerous paleoredox indices (PI) have been used in previous studies (e.g. Jones and Manning, 1994; Powell et al., 2003; Powell, 2009; McKirdy et al., 2011) to reconstruct the paleoredox conditions of ancient environments and sediments. These PIs include the ratios of the trace elements V/Cr, V/(V+Ni), U/Th, and Ni/Co, which are often used to determine the paleoredox conditions of marine shales. The PI V/(V+Ni) and V/Cr indices were utilized in the present study.

Because of its metamorphic history and age, reconstructing the paleoredox conditions of the Burgess Shale Formation in British Columbia, Canada, is difficult. Powell et al. (2003) geochemically analyzed the redox-sensitive trace element patterns of Mo, U/Th, V/Cr, V/(V+Ni), V/Sc, and Ni/Co from three sections of the Burgess Shale Formation as well as one section of the slightly younger Duchensay unit. Their results indicate oxic bottom water conditions for most beds of the Burgess Shale and Duchensay including horizons containing exceptionally preserved fossils (Powell, 2003). Localized anoxic horizons were found in the Burgess Shale such as troughs along the base of the Cathedral Escarpment. Powell et al. (2003) also found a lack of a major infaunal ecosystem as evident by common microbial mats maintaining an exaerobic paleoenvironment.

Powell (2009) compared geochemical analyses of the Burgess Shale and the Kinzers Shale of Pennsylvania, USA both middle Cambrian in age. The study geochemically analyzed the redox-sensitive elements Mo, Ni, Co, V, Sc, and the ratios of Ni/Co, V/Sc to reconstruct the paleoredox conditions of both BST deposits. The paleoredox geochemistry characteristics of the Kinzers Formation and the Walcott Quarry and Campsite Cliff of the Burgess Shale were broadly similar (Powell, 2009). Numerous beds within the Longs Park Member of the Kinzers Formation show dysoxic signals, suggesting deposition took place in sustained lower oxygen conditions.

In addition to redox-sensitive trace element analysis, Powell (2009) analyzed mineral features of the two shales to better understand paleoredox conditions. The presence of herringbone calcite and zoned quartz crystals in both shales is indicative of brines and may represent a commonality in the diagenetic environment of these two BST deposits. Powell (2009) concludes that BST preservation is not correlated with the specific dissolved oxygen content of bottom waters because several BST fossil beds in the Kinzers Shale were deposited in a fluctuating oxycline, while several BST fossil beds of the Burgess Shale indicate deposition under sustained oxygenated conditions. These results also suggest that bottom water oxygen levels do not correlate with increased exceptional preservation of fossils found in the Burgess Shale, Kinzers Shale, or other BST deposits (Powell, 2009).

The Emu Bay Shale of southern Australia is host to one of the richest BST deposits in the southern hemisphere. McKirdy et al. (2011) compared their findings on the bottom water paleoredox conditions of the Emu Bay Shale to that of other BST deposits. In order to reconstruct these paleoredox conditions, McKirdy et al. (2011) measured redox-sensitive trace element ratios of U/Th, V/Cr, Ni/Co, and V/Sc through 8 m of basal strata. Their

results suggest that deposition of the Lagerstätte took place in oxygenated waters and that suboxic or anoxic waters were not a prerequisite for this type of exceptional preservation (McKirdy et al., 2011). A lack of bioturbation is also observed in the Emu Bay Shale, which was thought to help maintain cyanobacterial mats and a sharp redox boundary at the sediment-water interface. The Burgess Shale has undergone more extensive thermal alteration in the form of greenschist facies metamorphism. For this reason, the Emu Bay Shale is suggested to be a more potentially useful source of information on BST preservation (McKirdy et al., 2011)

Kloss et al. (in review) geochemically analyzed multiple Cambrian BST deposits to determine if there existed a correlation between bioturbation and paleoredox conditions. Samples were collected and analyzed from the early Cambrian Maotianshan Shale (China), middle Cambrian Wheeler shale (USA), and the middle Cambrian Spence shale (USA). Kloss et al. (in review) measured and analyzed the ratios of V/Cr and V/(V+Ni) in addition to total organic carbon (TOC)/S, which can also be used as a reliable assessment of paleoredox conditions for all three deposits to reconstruct paleoredox conditions. Sampling was done on a 5-cm scale, and in one occurrence in the Spence shale on a 1-cm scale, to eliminate the possibility that sampling was too coarse to detect pulses of low oxygen bottom waters. Bioturbation levels in the three shale deposits were extremely low on average (ichnofabric index (ii) = ~1). Results of paleoredox geochemical analysis on all three deposits displayed consistent oxic bottom water conditions. These general results show that paleoredox conditions had little to no effect on bioturbation levels in these paleoenvironments (Kloss et al., in review).

Gaines (2014) criticizes this previous geochemical work by arguing that storm

deposits and event-driven sedimentation, which would wash in sediments and detrital skeletal material from an oxic source, helps to dilute any redox-sensitive trace element enrichment. Part of this argument is that redox-sensitive proxies are most effective when sedimentation is slow and continuous, while rapid event beds dominate BST deposits and alter the paleoredox geochemical signal in these settings (Gaines, 2014). Gaines and Droser (2010) were also critical of the coarse meter-scale sampling interval of most of these previous geochemical studies. This study addresses these criticisms by geochemically analyzing samples from both background sedimentation and event beds, as well as utilizing a fine cm-scale sampling interval.

### *2.3 The Indian Springs biota and correlative strata*

English and Babcock (2010) described exceptionally preserved fossils in the early Cambrian middle member of the Poleta Formation, Indian Springs Canyon, western Nevada, USA (Fig. 1). Exceptionally preserved BST fossils were found within three discontinuous intervals measuring less than one meter thick occurring at 20 m, 65 m, and 95 m above the base of the middle member (English and Babcock, 2010). The BST fossils were found in green and brown shales at the 20 m interval, gray and red shales in the 65 m interval, and gray shale at the 95 m interval (Fig. 2) (English and Babcock, 2010).

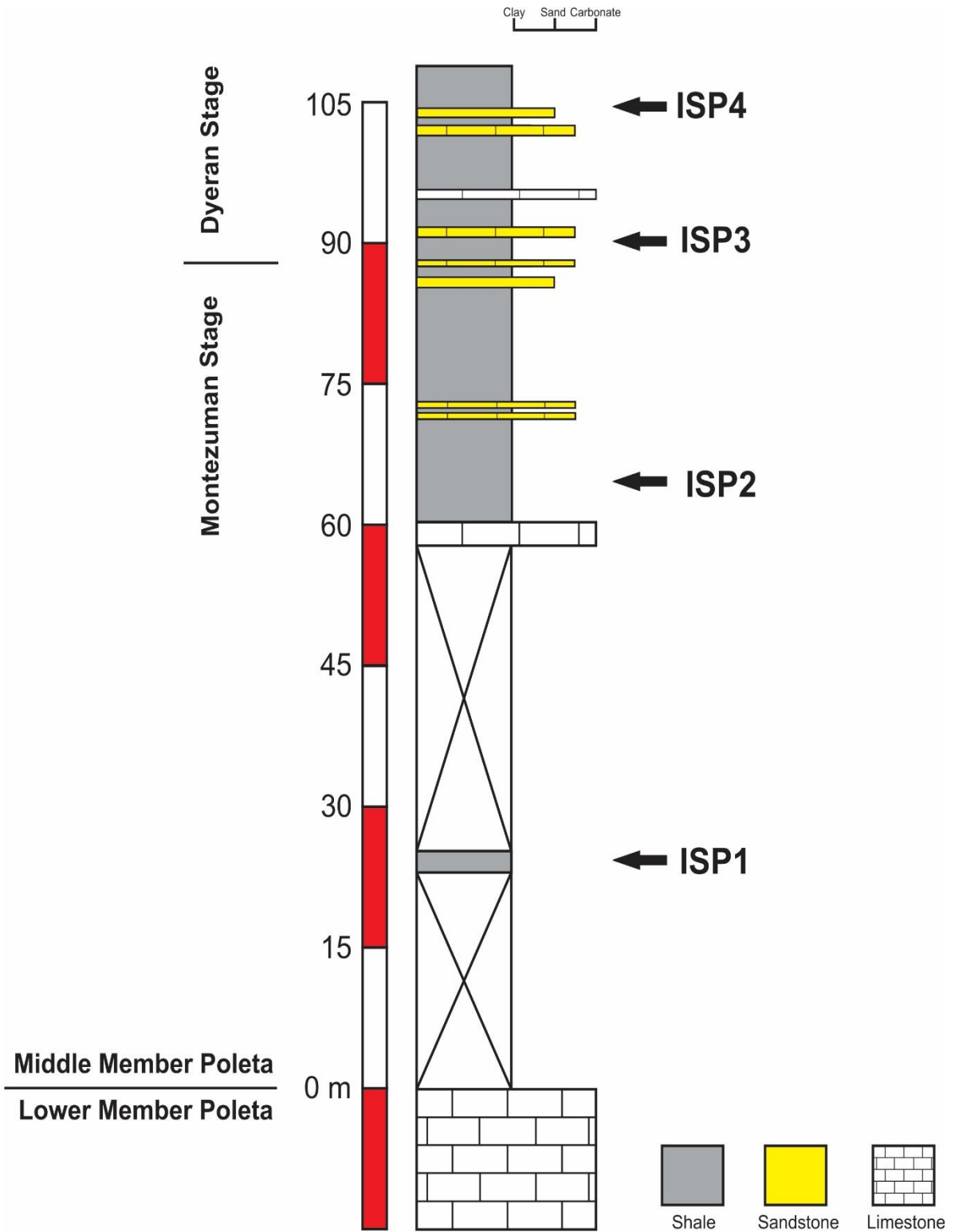


Figure 2 – Stratigraphic column (in meters) of Indian Springs locality showing the base of the middle member of the Poleta Formation. Arrows indicate sampling intervals.

The BST preservation intervals at 20 m and 65 m correspond to the basal flooding surfaces of three coarsening upward parasequences at this locality (English and Babcock, 2010). Shell beds and skeletal grainstones appear commonly in the lower portions of these parasequences. In other regions, these grainstones have been referred to as “base of parasequence shell beds” (Banerjee and Kidwell, 1991). Sedimentary structures such as hummocky cross stratification, bidirectional cross-bedding, and skeletal grainstones increase in frequency upwards in the parasequences (English and Babcock, 2010).

High abundances of both mineralized and non-mineralized animal fossils occur in these intervals in the middle member. Examples of non-mineralized fossils include brachiopods, demosponge skeletons, hyolithid gut tracts, mantle setae, trilobite appendages and digestive system parts (English and Babcock, 2010). These non-mineralized tissues were likely preserved through clay mineral replication, pyrite or iron oxide replication, or through retention of organic material (English and Babcock, 2010). Disarticulated biomineralized fossils found in adjacent strata include broken trilobite sclerites, inarticulate brachiopods, hyolithids, and helicoplacoid echinoderm ossicles. While a high abundance of fossils is present in the Indian Springs biota, it is relatively low in diversity when compared to similar-aged BST deposits. The Utah BST deposits, especially the Spence Shale, have perhaps the most similar biota to Indian Springs. Echinoderms and trilobites are relatively less common in the Chengjiang and Burgess Shale biotas (English and Babcock, 2010).

Ichnofossils in the Indian Springs biota are dominated by horizontal *Planolites* on the surfaces of bedding planes (English and Babcock, 2010). This is the most common trace fossil in the middle member of the Poleta Formation in both Nevada and California

(Marenco and Bottjer, 2008). Minimal horizontal bioturbation is observed at Indian Springs, with few examples of burrows penetrating deeper than one millimeter. Rare, discrete, and isolated burrows showing little to no disturbance of the original bedding (ii - 1-2) have been observed in cross-sectioned samples (English and Babcock, 2010).

In strata correlative to the Indian Springs biota, Dornbos and Bottjer (2000, 2001) analyzed the levels of bioturbation in helicoplacoid echinoderm-rich shales from a 12 m-thick interval of the middle member of the Poleta Formation in Westgard Pass, White-Inyo Mountains, eastern California (Fig. 1). Bioturbation in these samples is minimal and generally consists of horizontal *Planolites*. While the majority of the section displays low bioturbation levels (ii 1-2), a brief 5 cm section shows an ii of 3 (Dornbos and Bottjer, 2000). These strata correlate with the middle member of the Poleta Formation in the Montezuma Range, western Nevada (Fig. 1) because of the presence of rare helicoplacoid echinoderm fossils at both localities.

### **3. Geologic setting**

During the early Cambrian, what is now the western coast of North America was located along the northern coast of Laurentia within 30° of the Equator (Sundberg and McCollum, 1997). Because the coastline was a passive margin, deposition took place on a rather broad and shallow shelf (Fig. 3) (Moore, 1976). The Poleta Formation of eastern California and western Nevada is comprised of thick siliciclastic and carbonate dominated rocks, indicating a subsiding ramp throughout the span of the early Paleozoic (e.g. Robison, 1991).

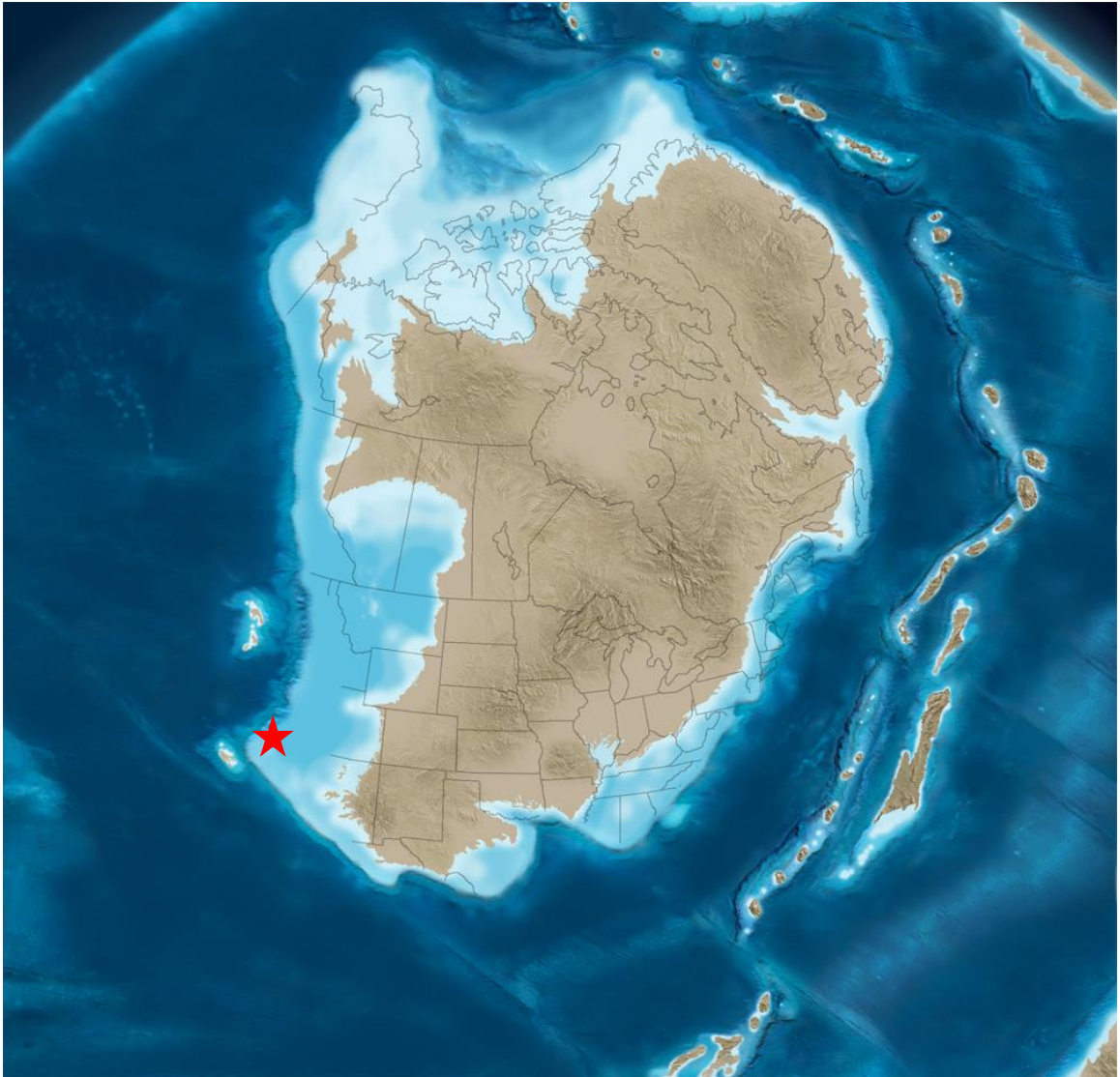


Figure 3 – Paleogeographic map of North America during the early Cambrian. Field site starred in red. From <http://jan.ucc.nau.edu/~rcb7/namC510.jpg>

Up to 125 m of the Poleta Formation is well exposed in Indian Springs Canyon in the northern part of the Montezuma Range, Esmeralda County, western Nevada (Figure 1), approximately 30 km southwest of Tonopah, Nevada (English and Babcock, 2010). The Poleta Formation is divided into lower, middle, and upper members (Fig. 1) (Stewart 1970; Hollingsworth, 1999, 2005; Streng et al., 2005). The primary focus of this study concerns the middle member, which is shale-dominated with thin interbeds of skeletal grainstones and thin-to-medium bedded sandstones (English and Babcock, 2010). The strata of the middle member are characteristic of a calm outer shelf paleoenvironment below normal wave base. Periodic high-energy obrution deposit event beds, comprised mostly of skeletal debris, are found interbedded within the calm, background sedimentation (Dornbos and Bottjer, 2001).

The middle member of the Poleta Formation represents a transition from a carbonate-bank depositional setting, as seen in the lower member, to terrigenous-dominated sedimentation on the outer shelf (Moore, 1976). The middle member ranges in thickness from 70 m to up to 230 m in some localities (Moore, 1976). Moore (1976) described four distinct units of the middle member in the White-Inyo Mountains, eastern California: A lower siltstone unit, a lower sandstone-siltstone unit, a middle limestone-siltstone unit, and an upper sandstone unit. The overlying upper member of the Poleta Formation represents a return to a carbonate-bank depositional environment (Moore, 1976).

The succession from the Campito Formation to the Poleta Formation represents a transgressive to highstand systems tract. This can be traced from the Montezuma Range westward into the White-Inyo Mountains of eastern California and southward into the

Mojave Desert and Death Valley (e.g. Hagadorn et al., 2000; Hollingsworth, 2005). The lower member of the Poleta Formation is mostly comprised of an oolitic grainstone, as well as archaeocyathan bioherms (e.g. McKee and Gangloff, 1969; Nelson, 1971), and represents lowstand systems tract deposition. The overlying 70 m to 230 m thick shale-dominated middle member records abrupt flooding of the shelf and is a transgressive to highstand systems tract.

No previous studies have examined the paleoredox geochemistry and bioturbation levels at the Indian Springs locality. The objective of the present study is to test these variable and assess whether or not either were controlling factors on observed BST preservation.

## **4. Methods**

### *4.1 Field methods*

Continuous *in situ* sections of rock were collected at the Indian Springs locality from outcrop at three horizons of previously documented BST preservation at the 20 m, 65 m, and 95 m intervals (See Appendices A and B) (English and Babcock, 2010) (sections ISP1, ISP2, and ISP3) above the base of the middle member of the Poleta Formation. The 20 m and 65 m localities were readily identified because of extensive previous quarrying activity. Another section was collected at the 105 m interval in order to serve as a control locality without BST preservation (ISP4). A total of 28 samples comprising 96.45 cm of strata were collected. Care was taken to sample unweathered rocks.

In order to generate random control samples, a square meter quadrat divided into 16 equal squares was randomly placed atop the talus debris at each of the four sampled

horizons. A random number generator was used to select one of the sixteen squares, from which a rock sample was taken. Five randomly selected samples were taken from the talus at each locality for a total of 20 samples. This method was used solely for geochemical analysis because of the lack of stratigraphic context. The geochemical data from these random quadrat samples serves as a control dataset for comparison to the *in situ* samples collected.

#### *4.2 Laboratory methods*

The 28 *in situ* samples were cut into three 1 cm thick slabs for: 1) XRF analysis; 2) X-radiograph analysis; and 3) petrographic thin section preparation (See Appendices C and D). Geochemical paleoredox proxies of the samples were calculated by measuring the abundances of the redox-sensitive trace metals V, Cr, and Ni, using X-Ray Fluorescence (XRF) and utilizing paleoredox indices (PIs). When measuring these trace metals, V/Cr ratios  $< 2.00$  indicates an oxic paleoenvironment (Fig. 4) - and V/(V+Ni) ratios  $> 0.84$  correlate to anoxic conditions (Jones and Manning, 1994; and Schovsbo (2001). These are the two PIs utilized for the present study.

<b>Auth U</b>	<b>U/Th</b>	<b>DOP</b>	<b>V/Cr</b>	<b>Ni/Co</b>	
12.00	1.25	0.75	4.25	7.00	← Suboxic - Anoxic
5.00	0.75	0.42	2.00	5.00	← Dysoxic
					← Oxic

Figure 4 – Chart displaying five paleoredox indices identified by Jones and Manning (1994) as most reliable. V/Cr is utilized for this study. Modified from Jones and Manning (1994).

Small samples (7-10g) of individual rock layers were powdered using a tungsten carbide shatterbox. The samples were dried in a drying oven overnight at 105°C. Loss on ignition (LOI) was calculated by heating samples (~1 g) of powdered rock to 1050°C in a muffled furnace for 15 minutes to drive off any volatile components. These powder samples were then fused into glass beads using a Claisse M4 fluxer. One gram of each powdered sample was then prepared as a glass bead using a 10:1 ratio of 50:50 Lithium Metaborate: Lithium Tetraborate flux:sample (with LiBr as a non-wetting agent) and 1 g of ammonium nitrate as an oxidizer, and then analyzed for major, minor, and select trace elements using a Bruker S4 Pioneer X-Ray Fluorescence Spectrometer (XRF) according to the same methodology as McHenry (2009). These methods were applied to all samples geochemically analyzed in this study. Concentrations of major and minor elements Si, Ti, Al, Fe, Mn, Mg, Ca, Na, K, P and trace elements Zr, Zn, Y, V, Sr, Ni, Nb, Ce, Cr, and Ba were determined and analyzed using a calibration based on eleven USGS igneous and sedimentary rock standards. To be considered detectable, an element's concentration must have been more than double the lower limit of detection and have a statistical error less than 12% for trace elements and 2% for major elements.

Thin sections were analyzed to interpret the depositional setting, sedimentological characteristics, and mm-scale bioturbation levels. Slabs were X-radiographed to analyze and interpret the bioturbation levels on a mm-scale through the stratigraphic sequences. The dominant microfacies was also recorded in thin sections and X-radiographs in order to determine if geochemical samples were being taken from event beds or background beds. The ichnofabric index (ii) method was utilized to measure bioturbation levels (Droser and Bottjer, 1986).

Nine samples from coeval strata of the middle member of the Poleta Formation from Westgard Pass, White-Inyo Mountains, eastern California (Fig. 2 in Dornbos and Bottjer, 2000) were also geochemically analyzed for PIs as a control group because of their lack of BST preservation. This locality correlates to the Indian Springs locality in the Montezuma Range, NV based on the presence of rare helicoplacoid echinoderm fossils at both localities. These data are used to help test whether bottom water paleoredox conditions are a controlling factor in BST preservation.

## 5. Results

### 5.1 Paleoredox geochemistry

Of the 28 *in situ* samples taken from the four horizons in the Indian Springs locality, nine contained non-detectable levels of the necessary redox-sensitive elements (see Appendix E) and could not be geochemically assessed for paleoredox conditions. These non-usable samples consist of all six samples from the 95 m horizon (ISP3) and all four samples from the 105 m horizon (ISP4). All remaining 18 samples from the 20 m and 65 m horizons have PI ratios indicative of oxic bottom water conditions throughout the Indian Springs locality of the Poleta Formation (Figs. 5 and 6). The values for the V/Cr PI range from 0.73 to 1.3, all well below the 2.0 threshold of oxic-dysoxic water conditions, thus indicative of oxic bottom water conditions. The values of the V/(V+Ni) PI range from 0.60 to 0.69, all below the 0.84 threshold indicative of oxic bottom waters (Figs. 5 and 6).

The 20 m locality (ISP1) contains nine samples. All nine samples give consistent oxic signals with V/Cr PI ranging from 0.73 to 1.3 (Fig. 5). This PI range is well below

the 2.0 threshold indicative of oxic bottom water conditions. The  $V/(V+Ni)$  PI range from 0.63 to 0.69, all below the 0.84 threshold indicative of oxic bottom waters. Evidence for oxic bottom water conditions is found throughout the 34.5 cm of strata at this locality.

The 65 m locality (ISP2) also yielded nine samples. The  $V/Cr$  PI range from 0.76 to 1.04, well below the 2.0 threshold indicative of oxic bottom water conditions (Fig. 6). The data from the  $V/(V+Ni)$  PI range from 0.61 to 0.67, all below the 0.84 threshold indicative of oxic bottom waters. While this PI cannot distinguish between dysoxic and oxic waters, it can clearly indicate the difference between anoxic and dysoxic bottom water conditions. When coupled with the  $V/Cr$  PI, it is evident that oxic bottom water conditions are found throughout the 20.9 cm of strata sampled at this locality.

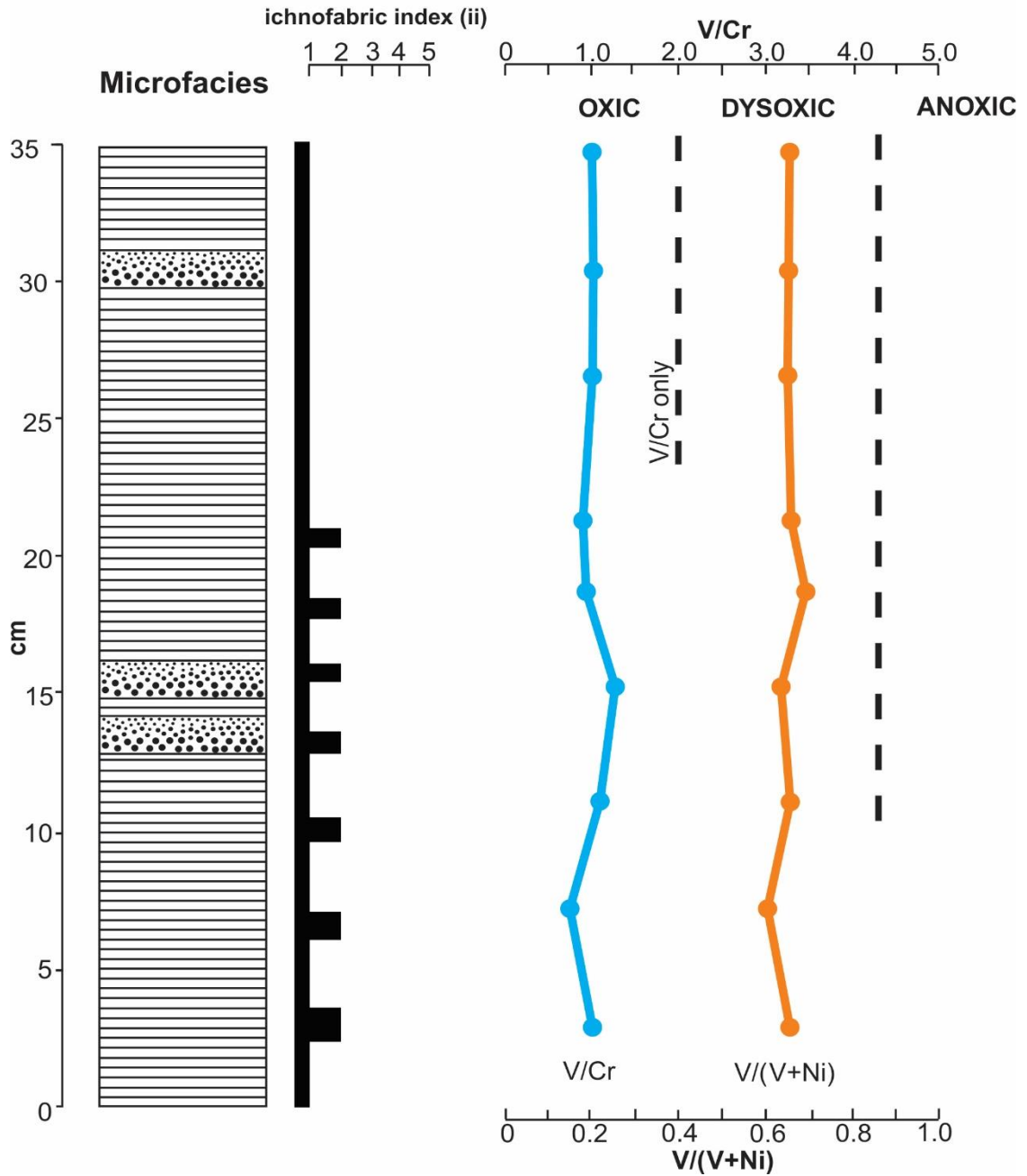


Figure 5 - Paleoredox indices ( $V/Cr$  and  $V/(V+Ni)$ ), ichnofabric indices, and microstratigraphy (event beds vs. background sedimentation) of the 20 m horizon (ISP1) at Indian Springs. Event beds are dotted intervals (graded beds). Background sedimentation is shown as thin lines (laminations).

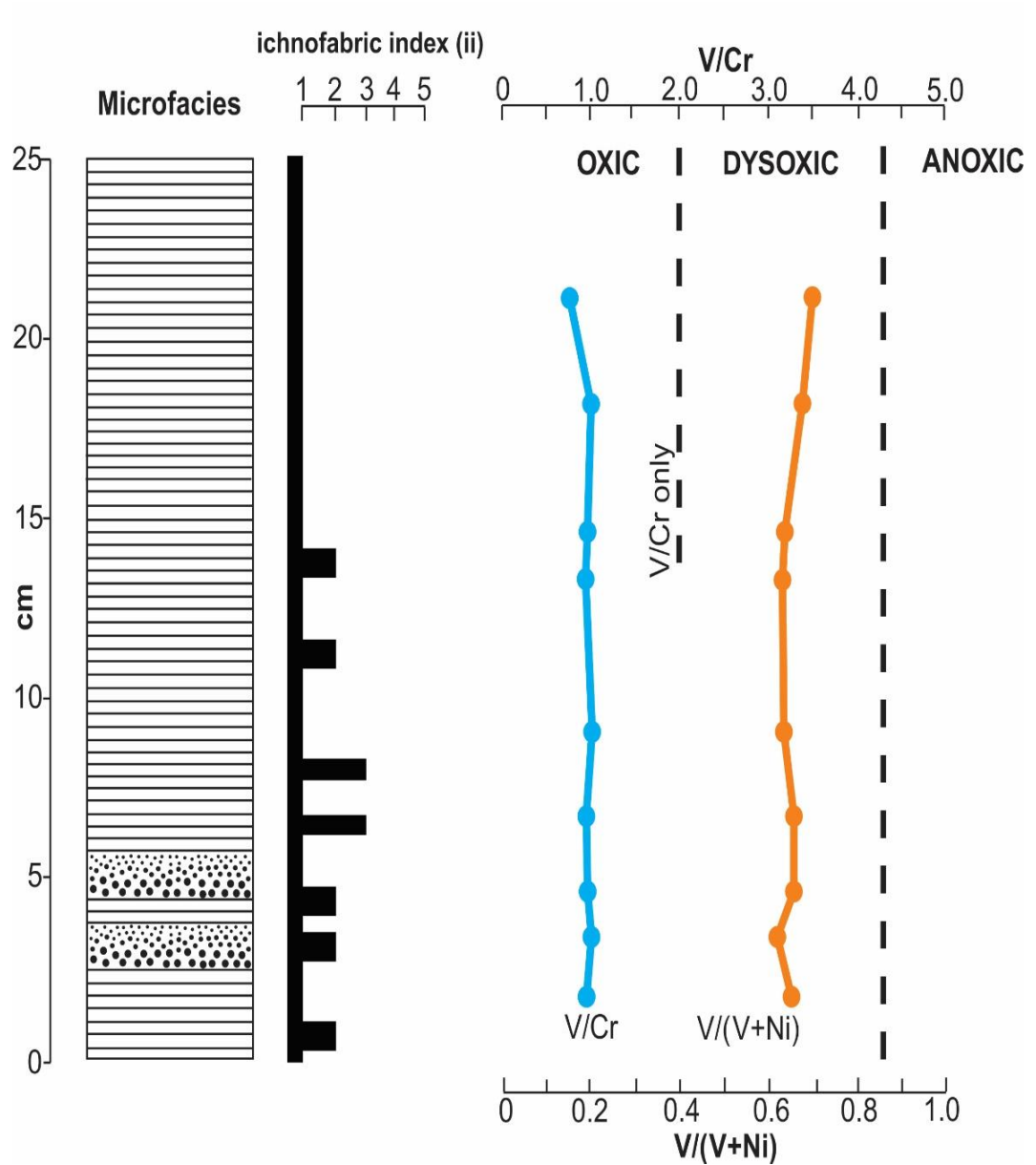


Figure 6 - Paleoredox indices ( $V/Cr$  and  $V/(V+Ni)$ ), ichnofabric indices, and microstratigraphy (event beds vs. background sedimentation) of the 65 m horizon (ISP2) at Indian Springs. Event beds are dotted intervals (graded beds). Background sedimentation is shown as thin lines (laminations).

The 20 samples collected using the quadrat method include eleven samples with non-detectable levels of redox-sensitive trace elements. All of the quadrat samples from the 105 m mark (ISP4) and all but one sample from the 95 m mark (ISP3) yield non-detectable levels of redox-sensitive trace elements (See Appendix E). The remaining nine samples from the 20 m and 65 m marks (ISP1 and ISP2) show oxic bottom water signals. The values of the V/Cr PI range from 0.78 to 1.47, below the 2.0 threshold indicative of oxic bottom waters. The V/(V+Ni) PI values range from 0.61 to 0.68, all below the 0.84 threshold indicative of oxic bottom waters (See Appendix E).

Eight of the nine White-Inyo Mountains samples contain detectable levels of the necessary redox-sensitive elements. These samples all yield oxic bottom water signals based on the paleoredox indices V/Cr and V/(V+Ni). The values of the V/Cr PI range from 0.76 to 1.09 and V/(V+Ni) values range from 0.63 to 0.75 (Fig. 7). Geochemical data from both of these localities are consistent with the those from the Maotianshan Shale, Spence Shale, and Wheeler Shale, as described by Kloss et al. (in review) (Fig. 8)

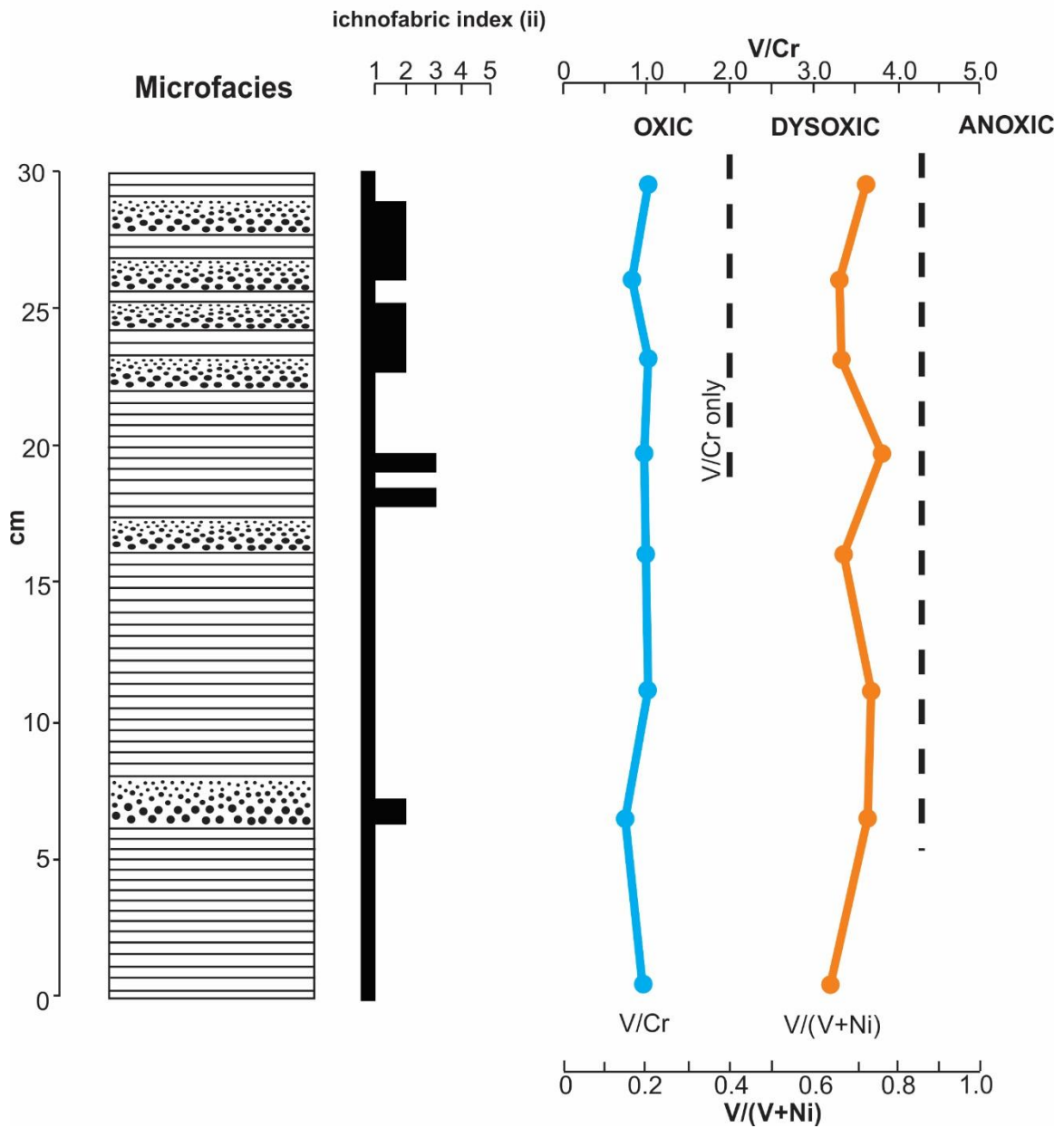


Figure 7 - Paleoredox indices (V/Cr and V/(V+Ni)), ichnofabric indices, and microstratigraphy (event beds vs. background sedimentation) of a section from the middle member of the Poleta Formation at Westgard Pass, White-Inyo Mountains, CA. Samples from Dornbos and Bottjer (2000). Event beds are indicated by dotted intervals (graded beds). Background sedimentation is shown as thin lines (laminations).

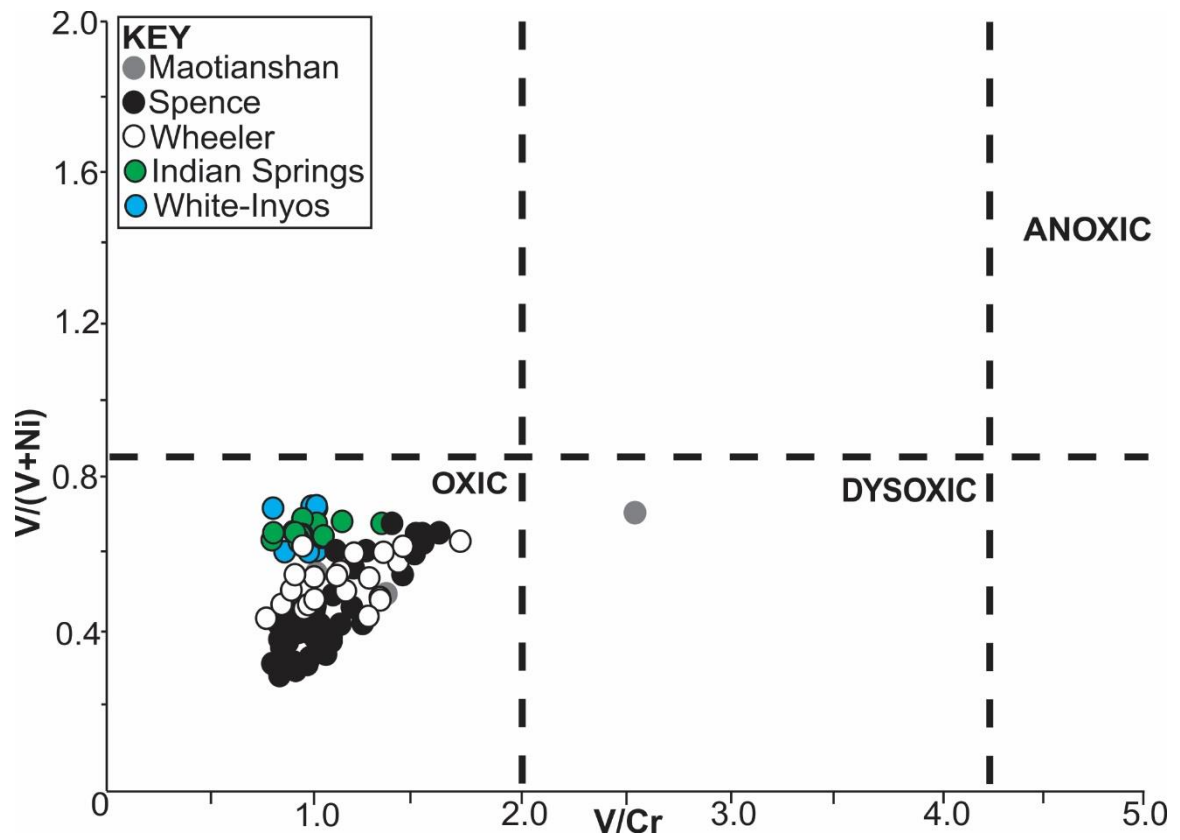


Figure 8 -  $V/Cr$  vs.  $V/(V+Ni)$  for the Poleta Formation at Indian Springs and White-Inyo Mountains. Data from Spence Shale, Wheeler Shale, and Maotianshan Shales from Kloss et al. (in review).

## 5.2 Bioturbation levels and microfacies

Bioturbation levels in both Indian Springs sample horizons with usable geochemical data are low (Figs. 5 and 6). In the 20 m horizon (ISP1) the *ii* is predominantly 1 throughout the 35 cm section, with brief appearances of *ii* of 2 in the lower 20 cm. The average *ii* at this locality is 1.21. At the 65 m locality (ISP2) the *ii* is also mostly 1 with brief appearances of *ii* 2-3 in the lower 15 cm of the section. The average *ii* at this locality is 1.38 (See Appendix F). All of the bioturbation observed at the Indian Springs locality occurs as horizontal *Planolites* burrows. No vertical bioturbation was observed.

Microfacies stratigraphy was observed on a mm-scale in thin sections and X-radiographs of samples from both the Indian Springs and White-Inyo Mountains localities. High-energy storm deposits, or event beds, were readily distinguished from thin-bedded background sedimentation (Figs. 9 and 10). The storm deposits are characterized by skeletal detrital material, likely transported from shallower areas above normal wave base. In the 35 cm of the 20 m section (ISP1) at the Indian Springs locality, three distinct storm deposit beds exist, at the 13 cm, 16 cm, and 31 cm marks in the section (Fig. 5). The strata in between these three horizons display fine-grained laminations consistent with background sedimentation. The 25 cm of strata observed at the 65 m horizon (ISP2) contains two thin event beds at the 3 cm and 5 cm marks in the section (Fig. 6). The event beds do not result in changes in the PI values for either of these localities (Figs. 5 and 6).

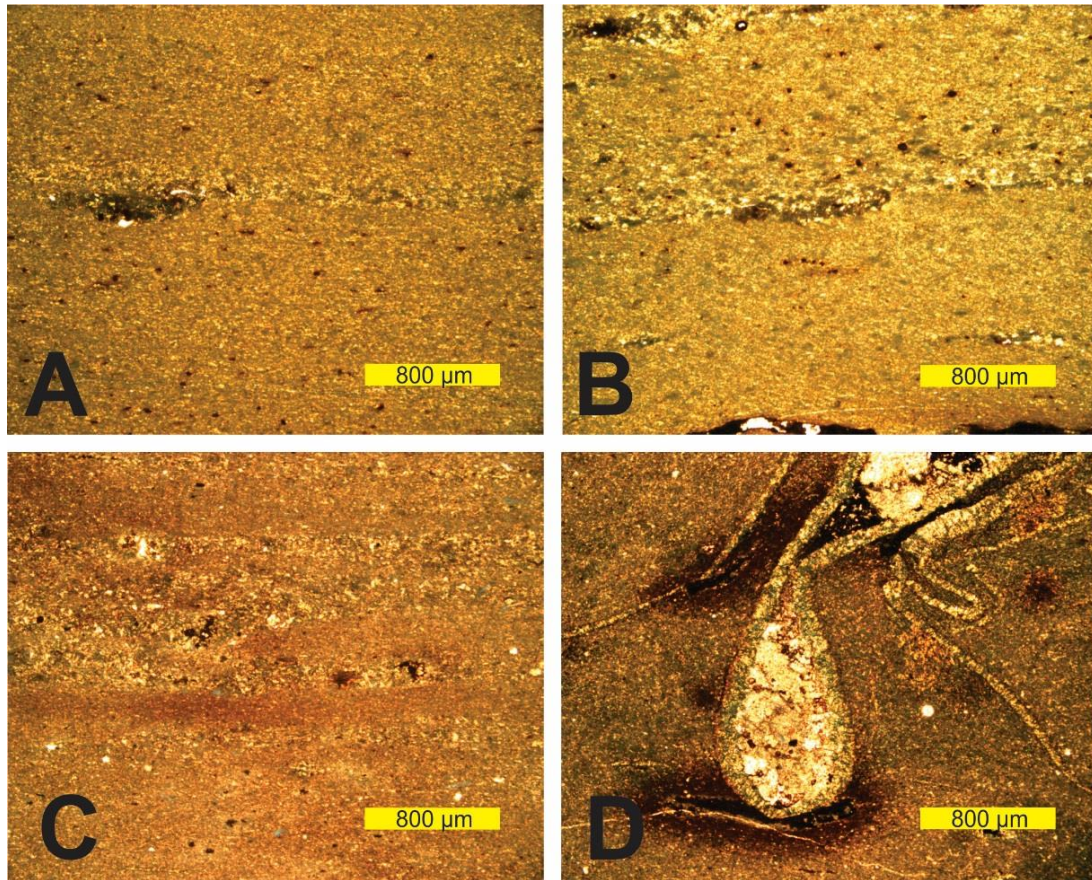


Figure 9 - Thin sections of rock from Indian Springs Canyon. In plain polarized light.  
A. ISP1-2, laminated bedding, B. ISP1-4, possible event bed, C. ISP2-3, laminated bedding of fine-grained sediment intermixed with coarser material, D. ISP2-4, trilobite skeletal material within an event bed.

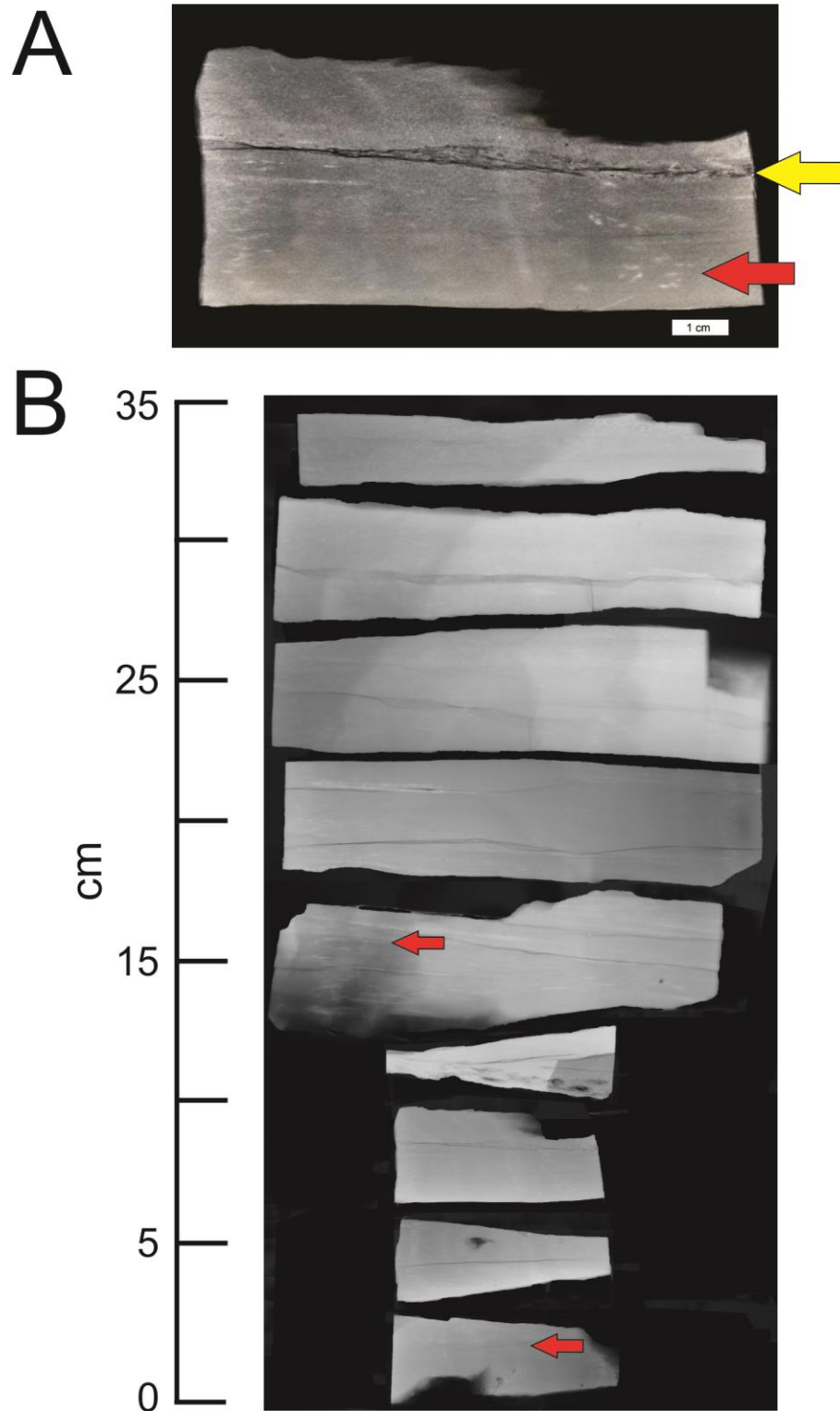


Figure 10 – X-radiographed slabs of rock samples from ISP1. A. Sample ISP1-6, yellow arrow indicating event bed, red arrow indicating bioturbation in the form of burrows. B. Red arrows indicating background laminations.

The bioturbation observed at the White-Inyo Mountains locality occurs as infrequent horizontal *Planolites* burrows (Dornbos and Bottjer, 2000, 2001), much like the Indian Springs locality. Within the 30 cm section, there are five horizons of skeletal detrital material, indicative of high-energy obrution deposits. These occur at the 7 cm, 17 cm, 23 cm, 25 cm, 27 cm, and 29 cm marks of the section (Fig. 7). The remaining strata are characterized by thinly laminated background sedimentation. There is more infaunal activity here compared to the Indian Springs locality, as documented by higher ii levels. There are two brief occurrences of ii-3 around the 18 cm mark and prolonged occurrences of ii-2 -between the 23 cm and 29 cm marks. The average ii is 1.55. Much as at Indian Springs, the presence of event beds does not influence PI values at this locality (Fig. 7).

## 6. Discussion

The paleoredox geochemistry of the Indian Springs biota indicates that it lived under an oxic water column. This is supported by data indicative of oxic bottom water conditions from the stratigraphically correlative White Inyo Mountains. Because there is no BST preservation at this locality despite similar paleoredox geochemistry, and the paleoredox geochemistry from the randomly selected talus samples at the Indian Springs locality also indicates oxic bottom water conditions, bottom water oxygenation does not appear to be a controlling factor in BST preservation. The results of this study therefore do not support the oxygen-restricted hypothesis for BST deposit formation.

The combination of low bioturbation levels and oxic paleoredox signals that conditions at Indian Springs are generally indicative of exaerobic conditions. The exaerobic zone is defined as having an oxic water column above a subsurface lacking a

major infauna or bioturbation separated by a sharp sediment-water interface (Savrda and Bottjer, 1987). These same characteristics are present in the stratigraphically coeval White-Inyo Mountain samples, and thus the benthic paleoenvironment there is interpreted as exaerobic as well. These results suggest a preliminary hypothesis that many Cambrian BST deposits, as well as some settings without BST preservation, exhibited exaerobic conditions during this time. In both the Indian Springs and White-Inyo localities, small event beds of skeletal material are present amidst thinly laminated background sedimentation. The PI values, however, do not change drastically from event beds to background sedimentation. Because PI values indicative of oxic signals are consistent throughout both localities, in both event beds and background sedimentation, we can reject the hypothesis of Gaines (2014) that the event beds transported the majority of redox-sensitive trace metals, thereby diluting the paleoredox signal.

All of the PIs in this study give consistent signals for deposition under oxic bottom waters (Fig. 8), regardless of whether BST preservation is present or not. Localized anoxic horizons may be present below the resolution of this study, so ephemeral oxygen fluctuations may have taken place. Previous paleoredox geochemical studies on the Cambrian BST deposits in the Burgess Shale, Kinzers Shale, Emu Bay Shale, Spence Shale, Wheeler Shale, and the Maotianshan Shale all show similar signatures of being deposited under largely oxic bottom water conditions, or at least fluctuating oxygen conditions in the Kinzers, despite low levels of bioturbation (Powell et al., 2003, Powell, 2009, McKirdy et al., 2011, Kloss et al. in review). These global data from multiple BST deposits indicate a clear, independent relationship between paleoredox conditions and bioturbation in these Cambrian paleoenvironments. This is in clear contrast to the co-

dependent relationship between the two observed in modern environments (Sturdivant, 2012).

In modern settings, extensive bioturbation and diverse burrows and trackways are coupled with abundant dissolved oxygen (Sturdivant, 2012). Conversely, when dissolved oxygen levels are low, bioturbation is minimal with trackways and burrows of low diversity. The lack of this relationship found in the present study suggests that paleoredox conditions were not a major controlling factor on bioturbation levels or BST preservation in Cambrian settings. Many models for BST preservation have anoxic or low-oxygen bottom waters as a prerequisite (e.g. Conway Morris, 1986; Butterfield, 1995; Petrovich, 2001; Butterfield, 2003; Gaines et al., 2005; and Gaines and Droser, 2010). This has led to the classic interpretation that many BST deposits were transported from oxygen-rich waters into an anoxic depositional setting for final burial. English and Babcock's (2010) findings indicate a clear and robust *in situ* ecosystem with BST preservation at Indian Springs, and this study suggests that oxic bottom water conditions made this possible.

Previous studies have proposed the roles of Fe-reducing bacteria (Petrovich, 2001), clay minerals (Butterfield et al., 1995), hypersaline brines (Calvert and Pederson, 1993), and the combination of anoxia, sulfate reduction, and low substrate permeability (Gaines et al., 2005) as possible mechanisms for the exceptional preservation observed in BST deposits. Further research on these variables could shed light on their roles in the BST preservation observed at Indian Springs Canyon.

## **7. Conclusions**

Geochemical analysis of paleoredox conditions using the PIs V/Cr and V/(V+Ni)

indicate oxic bottom water conditions at the time of deposition of both the exceptionally preserved Indian Springs biota and the stratigraphically correlative Poleta Formation locality in eastern California that lacks BST preservation. Bioturbation is low at the Indian Springs locality, with an average  $\lambda$  of 1.26. This suggests that a very minimal infauna was present and that mixed layer development was absent. In both the Indian Springs and Westgard Pass localities, burrows consist of horizontal *Planolites*. These characteristics indicate that exaerobic conditions existed in these paleoenvironments.

This study does not support the oxygen-restricted hypothesis of BST deposit formation. Bottom water paleoredox conditions do not appear to be a controlling factor on bioturbation levels or BST preservation in the Indian Springs biota. This indicates an independent relationship between bioturbation levels and bottom water paleoredox conditions during deposition of this unit. These results do support previous paleoredox geochemical studies on other Cambrian BST deposits that found evidence for oxic bottom water conditions, indicating that exaerobic conditions may have been pervasive in some paleoenvironments on Cambrian marine shelves.

## References

- Babcock, L.E., 2005. Interpretation of biological and environmental changes across the Neoproterozoic–Cambrian boundary: developing a refined understanding of the radiation and preservational record of early multicellular organisms. *Palaeogeography, Palaeoclimatology, Palaeoecology* 220, 1–5.
- Banerjee, I., Kidwell, S.M., 1991. Significance of molluscan shell beds in sequence stratigraphy: example from the Lower Cretaceous Manville Group of Canada. *Sedimentology* 38, 913–934.
- Bengtson, S., ed., 1994. *Early life on Earth*. Columbia University Press, New York, NY, 630 pp.
- Bottjer D.J., Droser, M.L. Jablonski, D., 1988. Paleoenvironmental trends in the history of trace fossils. *Nature* 333, 252-255.
- Bottjer, D.J., Hagadorn, J.W., Dornbos, S.Q., 2000. The Cambrian substrate revolution. *GSA Today* 10, 1-7.
- Butterfield, N.J., 1995. Secular distribution of Burgess Shale type preservation. *Lethaia* 28, 1-13.
- Butterfield, N.J., 2003. Exceptional fossil preservation and the Cambrian explosion. *Integrative and Comparative Biology* 43, 166-177 .
- Calvert, S.E. and Pederson, T.F., 1993. Geochemistry and recent oxic marine sediments: implications for the geological record. *Marine Geology* 113, 67-88.
- Ciarelli, S., Straalen, N.V., Klap, V.A., Wezel, A.P.V., 1999. Effects of sediment bioturbation by the estuarine amphipod *Corophium volutator* on fluoranthene resuspension and transfer into the mussel (*Mytilus edulis*). *Environmental Toxicology and Chemistry* 18, 318–328.
- Crimes, T.P., Fedonkin, M.A., 1994. Evolution and dispersal of deep-sea traces. *Palaios* 9, 74-83.
- Conway Morris, S., 1986. The community structure of the Middle Cambrian phyllopod bed (Burgess Shale). *Palaeontology* 29, 423-467.
- Dornbos, S.Q., Bottjer, D.J., 2000. Evolutionary paleoecology of the earliest echinoderms: Helicoplacoids and the Cambrian substrate revolution. *Geology* 28, 839-842.

- Dornbos, S.Q., and Bottjer, D.J., 2001. Taphonomy and environmental distribution of helicoplacoid echinoderms. *Palaios* 16, 197-204.
- Droser, M.L., Bottjer, D.J., 1986. A semiquantitative classification of ichnofabric. *Journal of Sedimentology Petrology*, 56, 558–559.
- Droser, M.L., Gehling, J.G., Jensen, S., 1999. When the worm turned: Concordance of Early Cambrian ichnofabric and trace-fossil record in siliciclastic rocks of South Australia. *Geology* 27, 625-628.
- English, A.M., Babcock, L.E., 2010. Census of the Indian Springs Lagerstätte, Poleta Formation (Cambrian), western Nevada, USA. *Palaeogeography, Palaeoclimatology, Palaeoecology*, 295, 236-244.
- Gaines, R.R., 2014. Burgess Shale-type preservation and its distribution in space and time. In: Laflamme, M., Schiffbauer, J.D., and Darroch, S.A.F. (Eds.), *Reading and writing of the fossil record: Preservation pathways to exceptional fossilization: The Paleontological Society Papers*, 20, 123–146.
- Gaines, R.R., Droser, M.L. 2010. The paleoredox setting of Burgess Shale-type deposits. *Palaeogeography, Palaeoclimatology, Palaeoecology* 297, 649-661.
- Gaines, R.R., Kennedy, M.J., Droser, M.L., 2005. A new hypothesis for organic preservation of Burgess Shale taxa in the middle Cambrian Wheeler Formation, House Range, Utah. *Palaeogeography, Palaeoclimatology, Palaeoecology*, 220, 193-205.
- Garson, D.E., Gaines, R.R., Droser, M.L., Liddell, W.D., Sappenfield, A., 2012. Dynamic paleoredox and exceptional preservation in the Cambrian Spence Shale of Utah. *Lethaia* 40, 164-177.
- Gehling, J.G., 1986. Algal binding of siliciclastic sediments: A mechanism in the preservation of Ediacaran fossils: 12<sup>th</sup> International Sedimentological Congress, Canberra, Australia, Abstracts, p. 117.
- Gehling, J.G., 1996. Taphonomy of the terminal Proterozoic Ediacaran biota, South Australia. Ph.D. thesis, University of California, Los Angeles, pp. 222.
- Gould, S.J., 1989. *Wonderful Life*. W.W. Norton, New York, p 347.
- Hagadorn, J.W., Bottjer, D.J., 1997. Wrinkle structures: microbially mediated sedimentary structures common in subtidal siliciclastic settings at the Proterozoic-Phanerozoic transition. *Geology* 25, 1047-1050.
- Hagadorn J.W., Schellenberg, S.A., Bottjer, D.J., 2000a. Paleoecology of a large Early Cambrian bioturbator. *Lethaia* 33, 142-156.

Hagadorn, J.W., Fedo, C.M., Waggoner, B.M., 2000b. Early Cambrian Ediacaran-type fossils from California. *Journal of Paleontology*, 74, 731-740.

Hagadorn, J.W., 2002. Chengjiang: Early record of the Cambrian explosion. In: Bottjer, D.J., et al., (Ed.), *Exceptional Fossil Preservation: A Unique View on the Evolution of Marine Life*. Columbia University Press, pp. 35-60.

Hollingsworth, J.S., 1999. Stop 11: Proposed stratotype section and point for the base of the Dyeran stage. In: Palmer, A.R (Ed.), *Laurentia 99, V Field Conference of the Cambrian Stage Subdivision Working Group*. International Subcommission on Cambrian Stratigraphy, pp. 38–42.

Hollingsworth, J.S., 2005. The earliest occurrence of trilobites and brachiopods in the Cambrian of Laurentia. *Palaeogeography Palaeoclimatology Palaeoecology* 220, 153–165.

Jones, B. Manning, D.A.C., 1994. Comparison of geochemical indexes used for interpretation of paleoredox conditions in ancient mudstones. *Chemical Geology* 111, 111-129.

Kloss, T.J., Dornbos, S.Q., Chen, J.Y., McHenry, L.J., Marengo, P.J., in review. High-resolution geochemical evidence for oxic bottom waters in multiple Cambrian Burgess Shale-type deposits. *Earth and Planetary Science Letters*, 27 ms pp.

Landing, E., 2001. “Burgess biotas” and episodic slope and epicontinental sea dysaerobia in the late Precambrian-Paleozoic. *Geological Society of America Annual Meeting Abstracts with Programs*, vol. 33, p. 38.

Marengo, K.N., and Bottjer, D.J., 2008. The importance of Planolites in the Cambrian substrate revolution. *Palaeogeography, Palaeoclimatology, Palaeoecology* 258, 189–199.

McHenry, L.J., 2009. Element mobility during zeolitic and argillic alteration of volcanic ash in a closer-basin lacustrine environment: Case study Olduvai Gorge, Tanzania. *Chemical Geology* 265, 540-532.

McKirdy, D.M., Hall, P.A., Nedin, C., Halverson, G.P. Michaelsen, B.H., Jago, J.B., Gehling, J.G., Jenkins, R.J.F., 2011. Paleoredox status and thermal alteration of the lower Cambrian (Series 2) Emu Bay shale Lagerstätte, South Australia. *Australian Journal of Earth Sciences* 58, 259-272.

McIlroy, D., Heys, G.R., 1997. Palaeobiological significance of *Plagiogmus arcuatus* from the Lower Cambrian of central Australia. *Alcheringa* 21, 161-178.

McKee, E.H., and Gangloff, R.A., 1969. Stratigraphic distribution of Archaeocyathids in the Silver Peak Range and the White and Inyo Mountains, western Nevada and eastern California. *Journal of Paleontology* 43, 716-726.

- McLennan, S.M., 2001. Relationships between the trace element composition of sedimentary rocks and upper continental crust. *Geochemistry, Geophysics, Geosystems* 2 (paper # 2000GC000109).
- Moore, J.N., 1976. Depositional environments of the Lower Cambrian Poleta formation and its stratigraphic equivalents. *Brigham Young University Geology Studies* 23, 23-28.
- Nelson, C.A., 1971. Geologic map of the Waucoba Spring Quadrangle, Inyo County, California, U.S. Geological Survey Map GQ, p. 921.
- Petrovich, R., 2001. Mechanisms of fossilization of the soft-bodied and lightly armored faunas of the Burgess Shale and of some other classical localities. *American Journal of Science* 301, 682-726.
- Powell, W., 2009. Comparison of geochemical and distinctive mineralogical features associated with the Kinzers and Burgess-Shale formations and their associated units. *Palaeogeography, Palaeoclimatology, Palaeoecology*, 227, 127-140.
- Powell, W.G., Johnston, P.A., Collum, C.J., 2003. Geochemical evidence for oxygenated bottom waters during deposition of fossiliferous strata of the Burgess Shale Formation. *Palaeogeography, Palaeoclimatology, Palaeoecology* 201, 249-268.
- Robinson, R.A., 1991. Middle Cambrian biotic diversity: examples from four Utah Lagerstätten. In: Simonetta, A.M., Conway Morris, S. (Eds.), *The early evolution of Metazoa and the significance of problematic taxa*. Cambridge University Press, Cambridge, pp. 77-98.
- Savrda, C.E., Bottjer, D.J., 1987. The exaerobic zone, a new oxygen-deficient marine biofacies. *Nature* 327, 54-56.
- Schieber, J., 1986. the possible role of benthic microbial mats during the formation of carbonaceous shales in shallow Mid-Proterozoic basins. *Sedimentology* 33, 521-536.
- Schovsbo, N.H., 2001. Why barren intervals? A taphonomic case study of the Scandinavian Alum Shale and its faunas. *Lethaia* 34, 271-285.
- Seilacher, A., Pflüger, F., 1994. From biomats to benthic agriculture: A biohistoric revolution. In: Krumbein, W.E., Paterson, D.M., Stal, L.J. (Eds.), *Biostabilization of sediments: Oldenburg, Germany, Bibliotheks und Informations-system der Carl von Ossietzky Universität Oldenburg*, pp. 97-105.
- Stewart, J.H., 1970. Upper Precambrian and Lower Cambrian strata in the southern Great Basin, California and Nevada. *US Geological Survey Professional Papers*, vol. 620, pp. 1-206.

- Streng, M., Babcock, L.E., Hollingsworth, J.S., 2005. Agglutinated protists from the lower Cambrian of Nevada. *Journal of Paleontology* 79, 1214–1218.
- Sturdivant, S.K., Diaz, R.J. & Cutter, G.R., 2012. Bioturbation in a declining oxygen environment, *in situ* observations from Wormcam. *PLoS ONE* 7, 1-11.
- Sundberg, F.A., McCollum, L.B., 1997. Oryctocephalids (Corynexochida: Trilobita) of the lower-Middle Cambrian boundary interval from California and Nevada. *Journal of Paleontology* 71, 1065-1090.
- Tribovillard, N., Algeo, T.J., Riboulleau, A., 2006. Trace metals as paleoredox and paleoproductivity proxies: an update. *Chemical Geology* 232, 12-32.
- Tyson, R.V., Pearson, T.H., 1991. Modern and ancient continental shelf anoxia: an overview. In: Tyson, R.V., Pearson, T.H. (Eds.), *Modern and Ancient Continental Shelf Anoxia*. Geological Society Special Publications 58, 1-26.
- Vermeij, G.J., 1989. The origin of skeletons. *Palaios* 4, 585-589.
- Wedepohl, K.H., 1971. Environmental influences on the chemical composition of shales and clays. In: Ahrens, L.H., Press, F., Runcorn, S.K., Urey, H.C. (Eds.), *Physics and Chemistry of the Earth*. Pergamum, Oxford, pp. 305–333.
- Wedepohl, K.H., 1991. The composition of the upper Earth's crust and the natural cycles of selected metals. In: Merian, E. (Ed.), *Metals and their Compounds in the Environment*. VCH-Verlags- gesellschaft, Weinheim, pp. 3–17.

**Appendix A:**

**Photos of Field Location at Indian Springs Canyon, NV**

Middle Member, Poleta Formation, Indian Springs Canyon, NV from where sections were sampled.



Terrain of field location at Indian Springs Canyon, NV (looking east).



Quadrat used to randomly sample talus samples.



Sampling location of 20 m section (ISP1), hammer for scale.



Sampling location of 65 m section (ISP2).



Sampling location of 95 m section (ISP3), hammer for scale.



Outcrop exposed at the 105 m location (ISP4).



Hummocky cross stratification sedimentary structure observed at approximately the 105 m section (ISP4), lens cap for scale.



**Appendix B:**  
**Table of Detailed Locality Information**

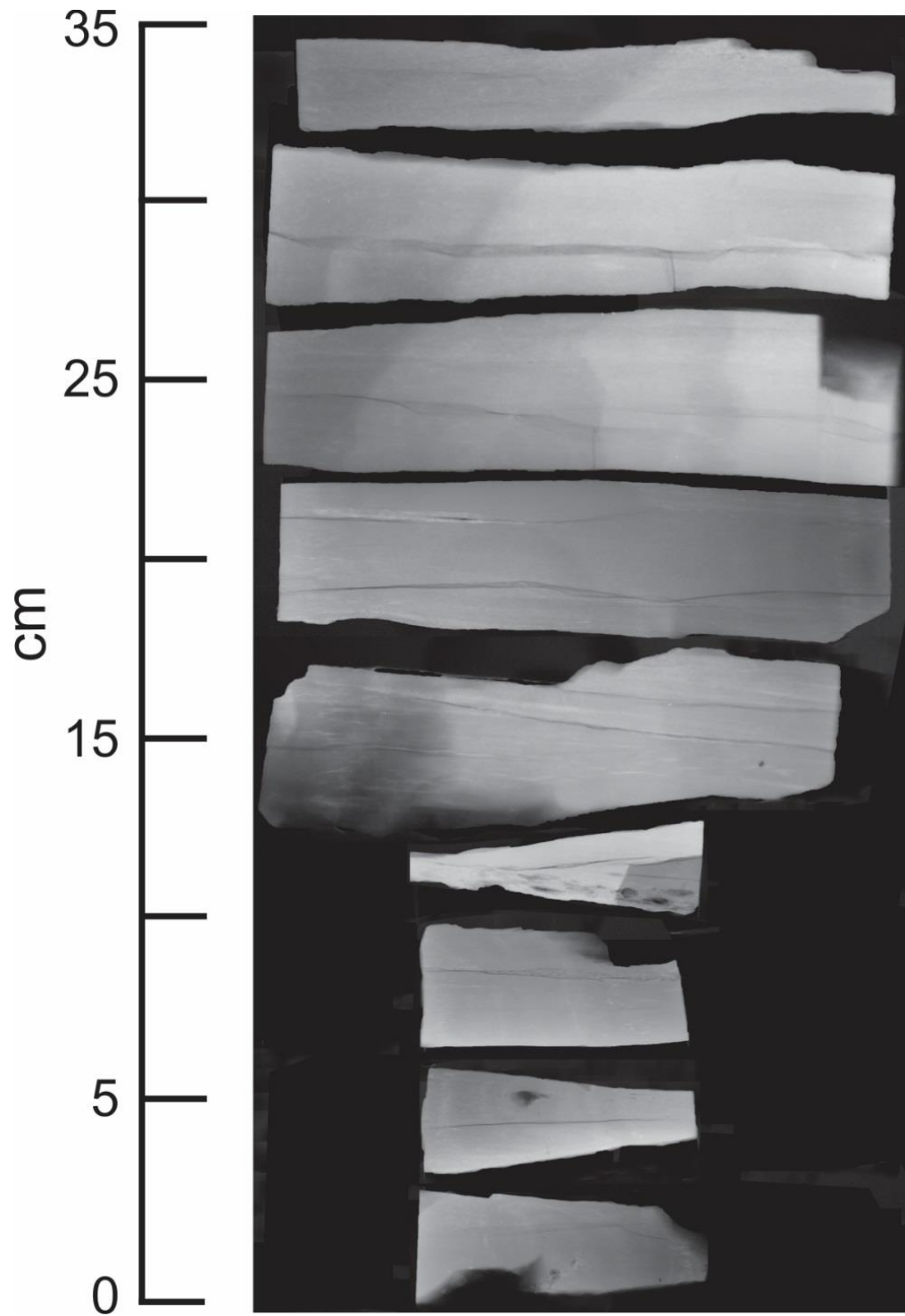
---

<b>Location</b>	<b>GPS Coordinates</b>
ISP1 (20 m)	N 37° 43.488, W 117° 19.186
ISP2 (65 m)	N 37° 43.391, W 117° 19.296
ISP3 (95 m)	N 37° 43.384, W 117° 19.330
ISP4 (105 m)	N 37° 43.372, W 117° 19.357
WP-WI	N 37° 17.45, W 118° 08.15

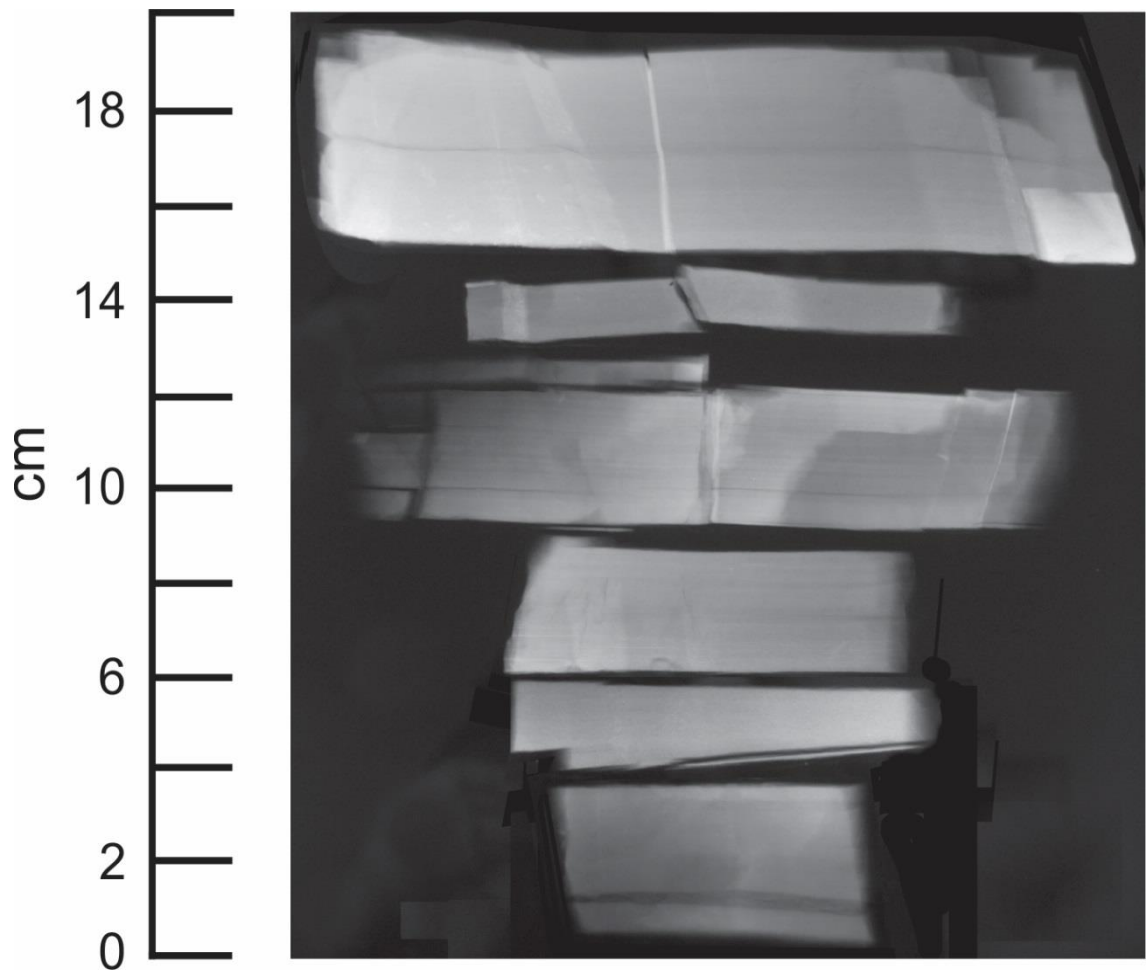
ISP = Indian Springs Canyon, NV. WP-WI = Westgard Pass, White-Inyo Mountains, CA

**Appendix C:**  
**X-radiograph Images**

X-radiograph composite column of samples from ISP1.



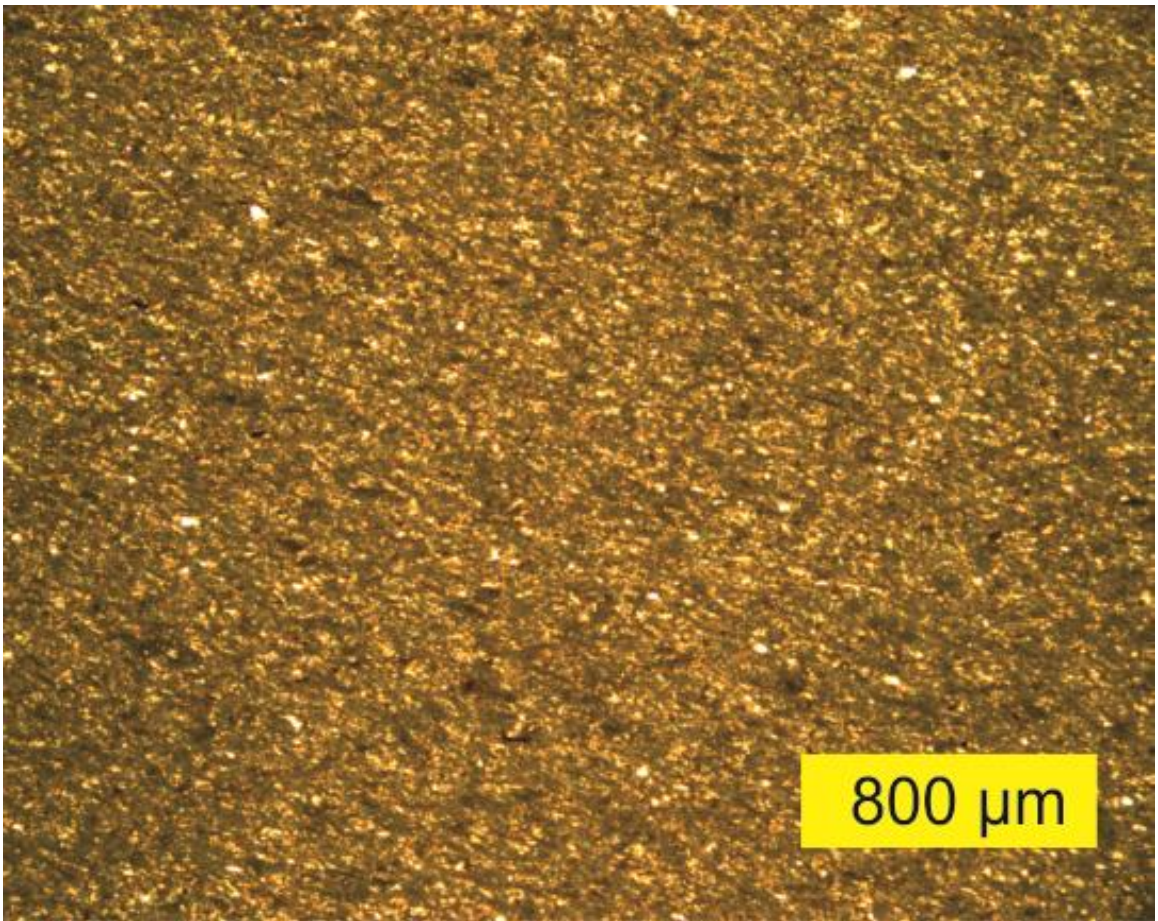
X-radiograph composite column of samples from ISP2.



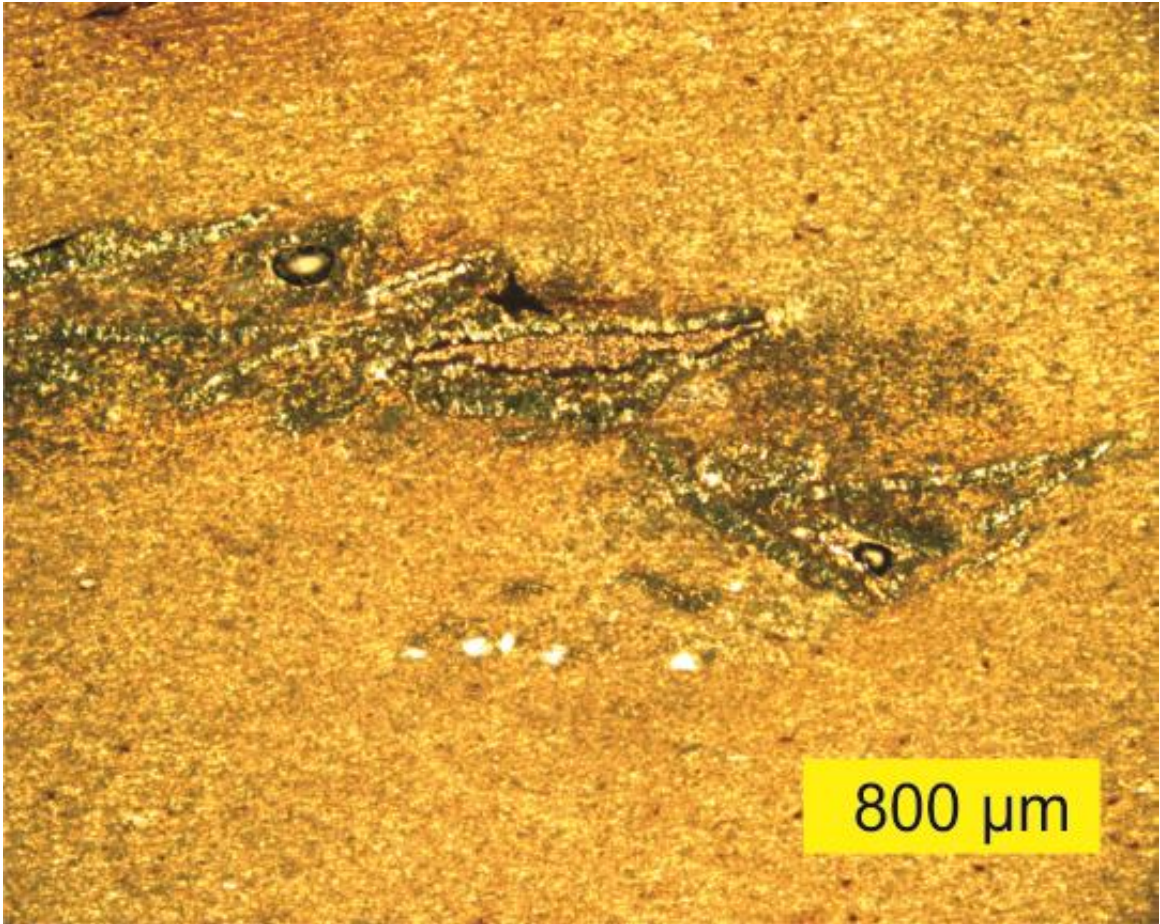
**Appendix D:**

**Thin Sections From ISP1 and ISP2 in Plane Polarized Light**

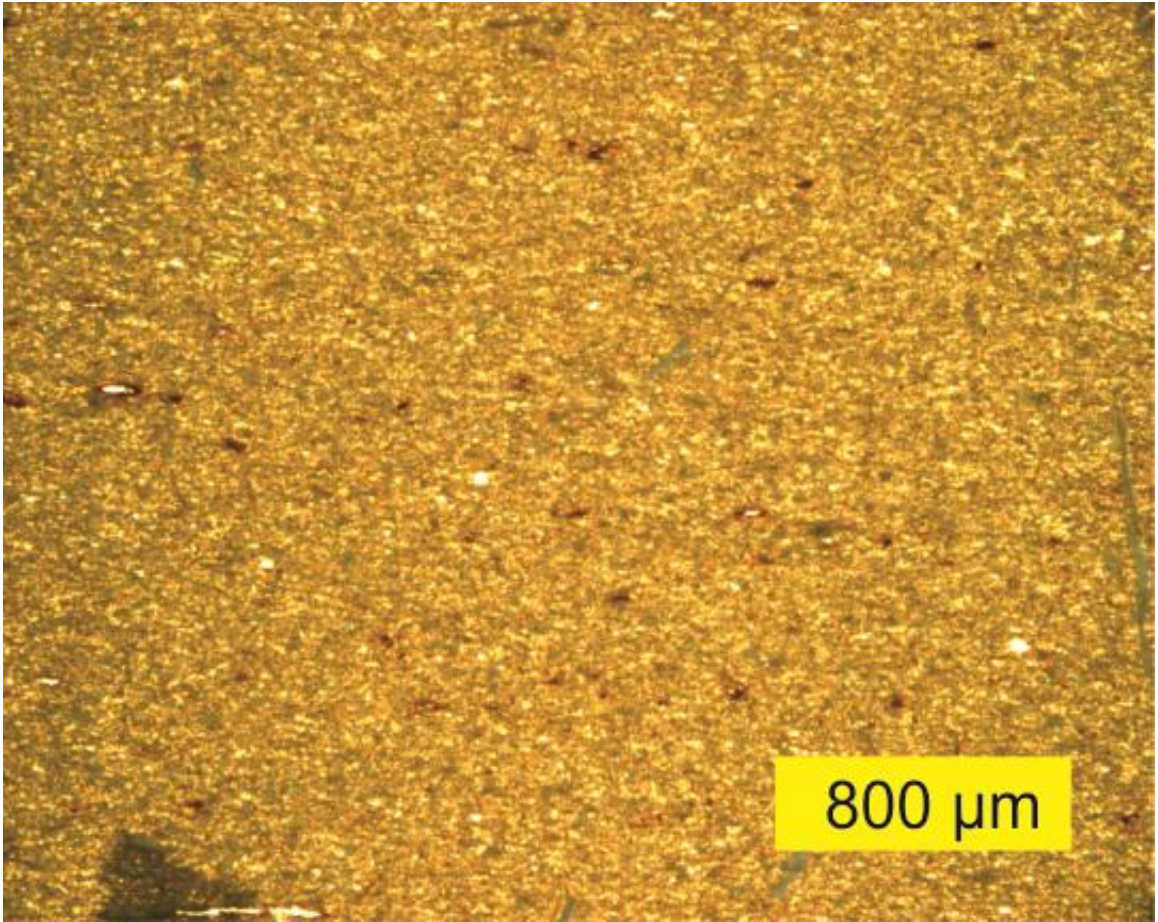
Sample ISP1-1B,



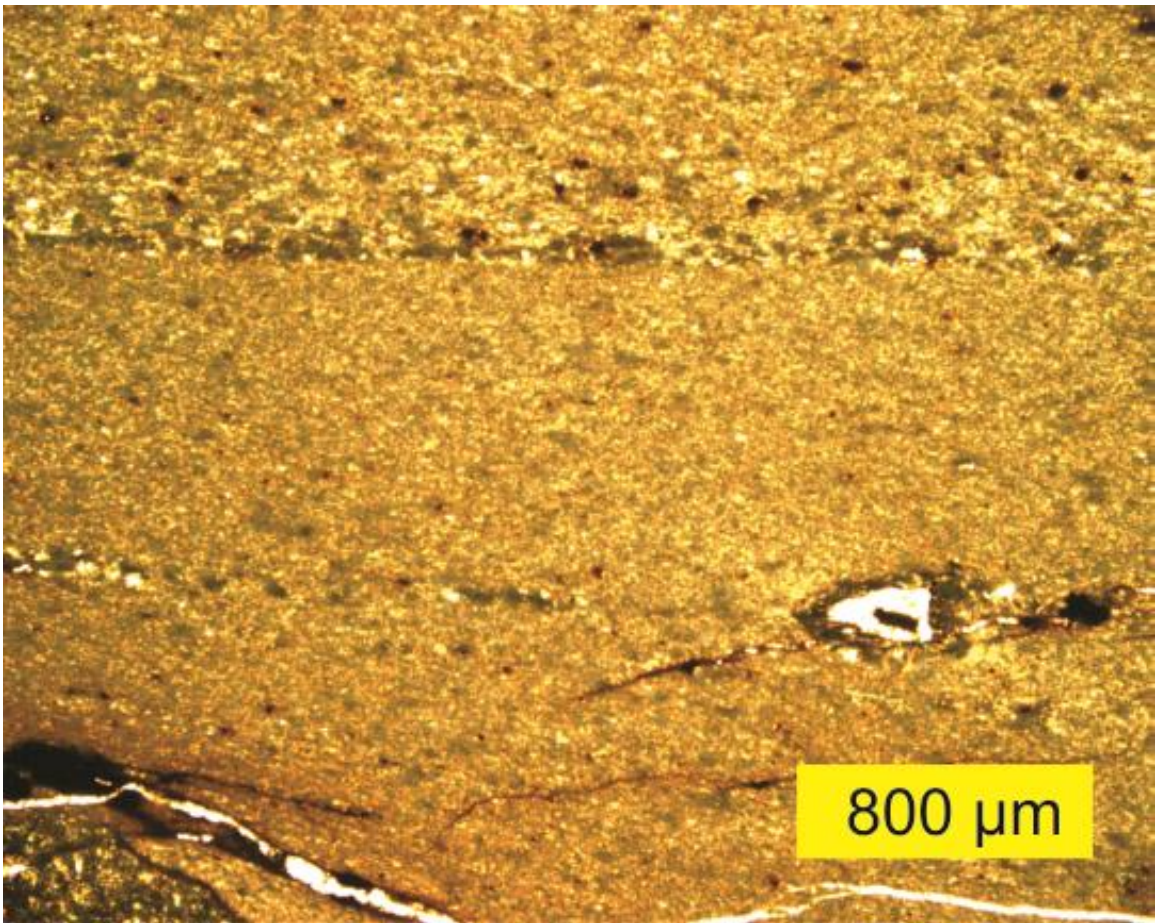
Sample ISP1-2



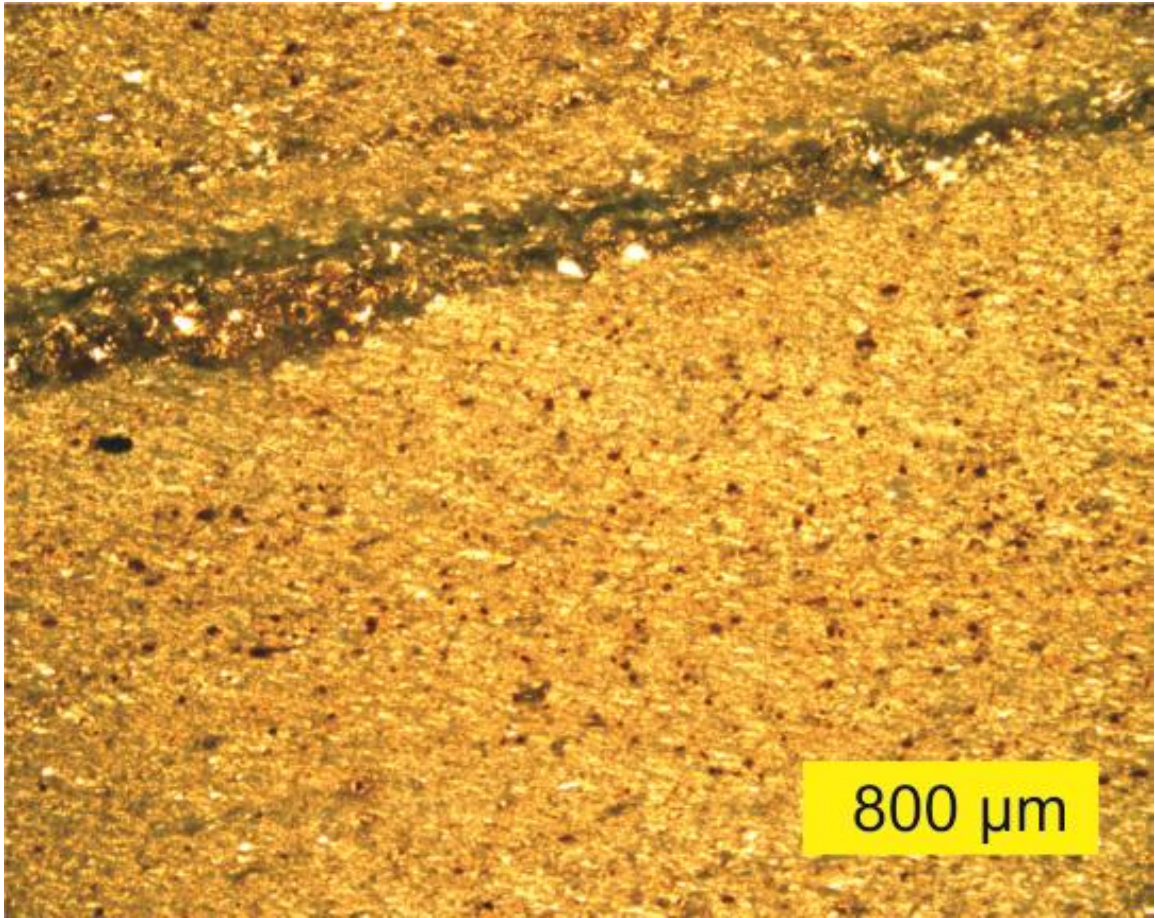
Sample ISP1-3



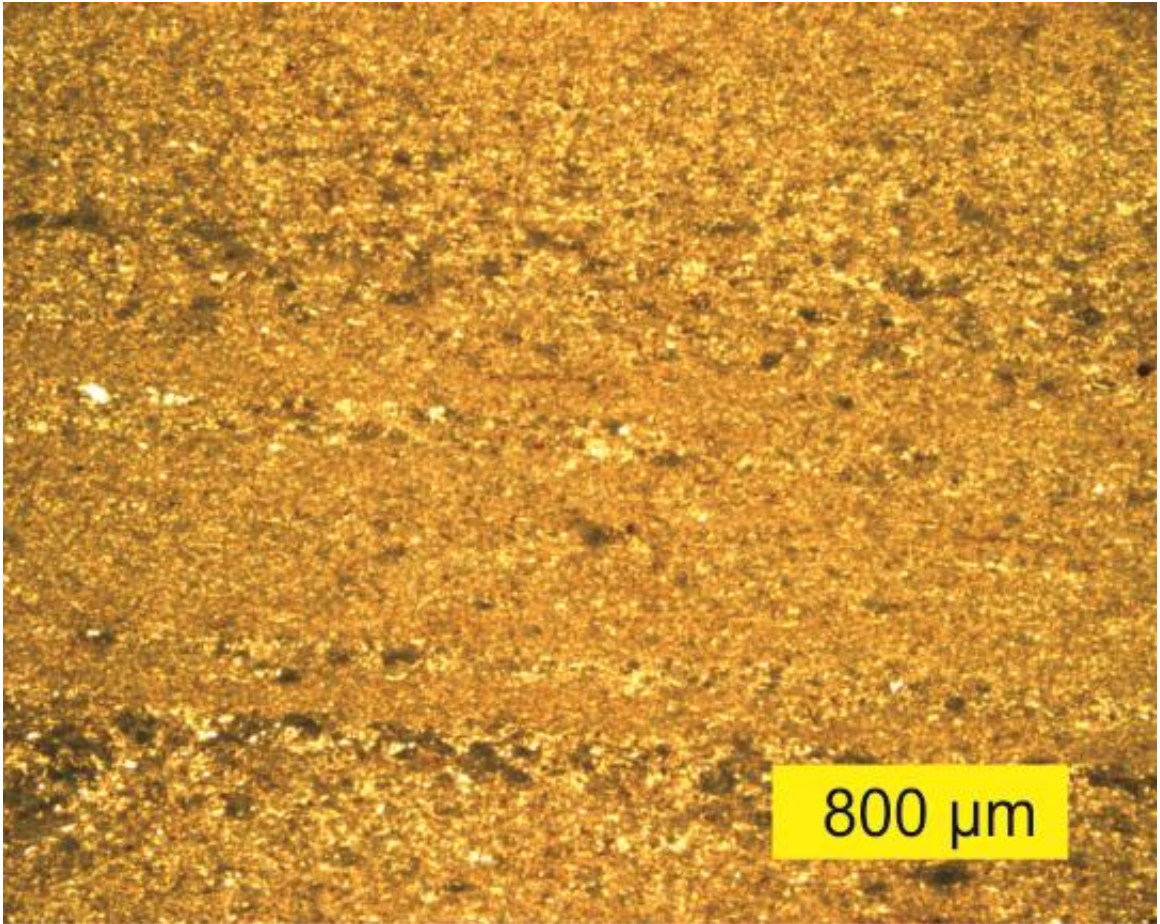
Sample ISP1-4



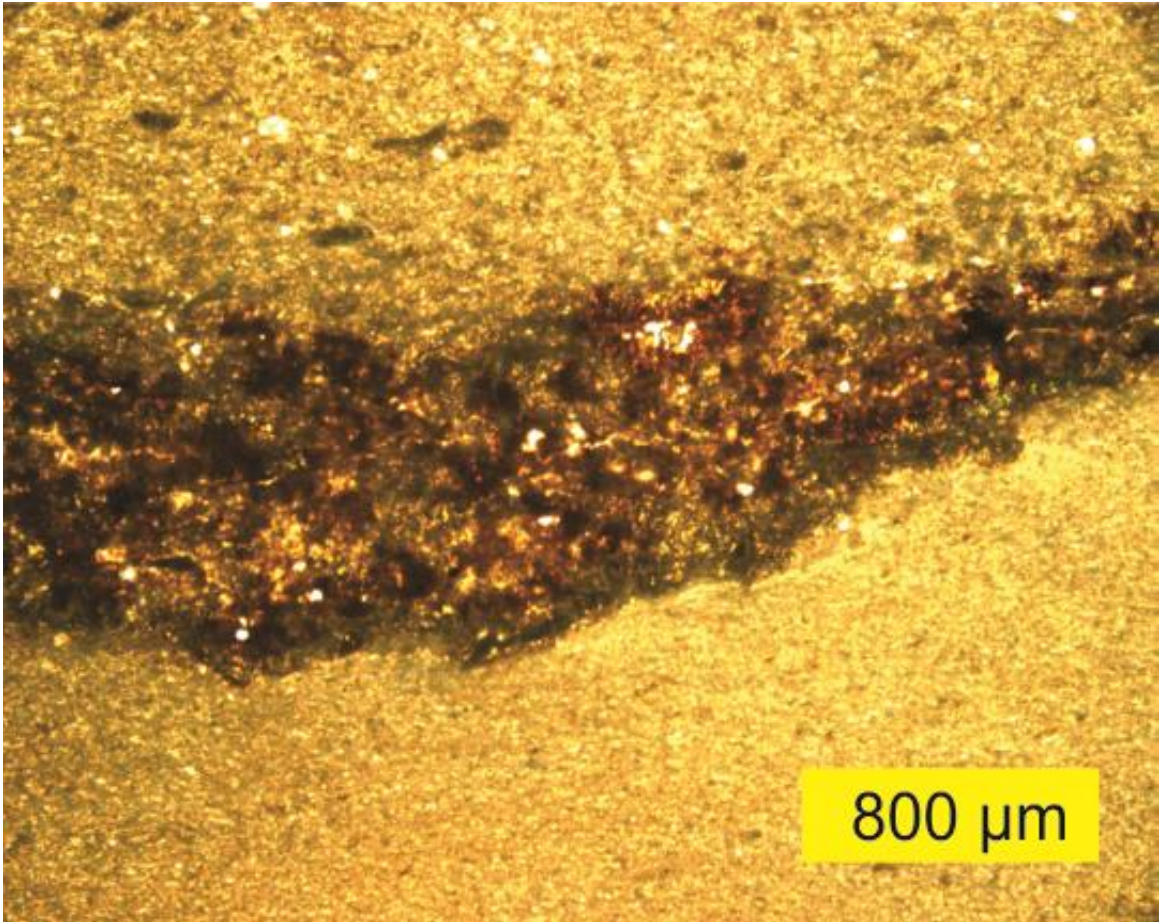
Sample ISP1-5



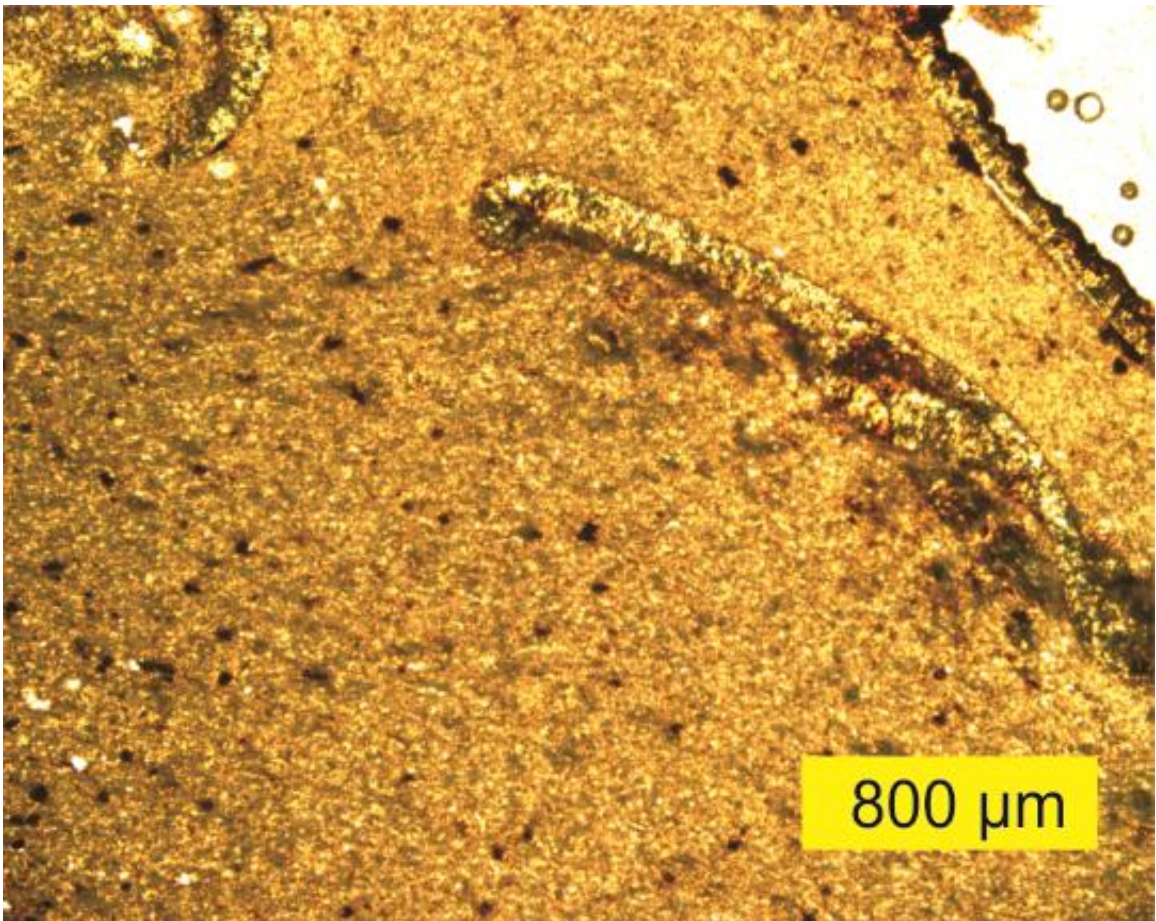
Sample ISP1-6



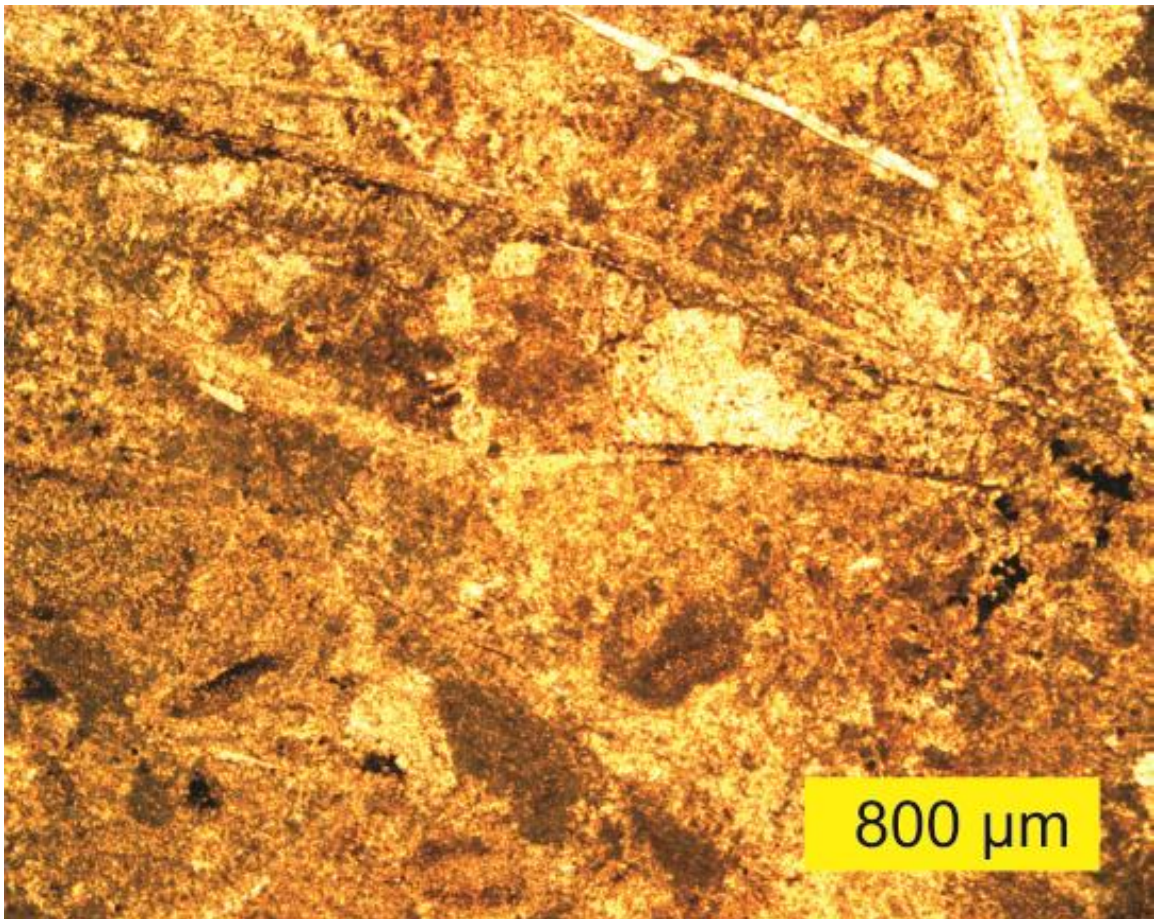
Sample ISP1-7



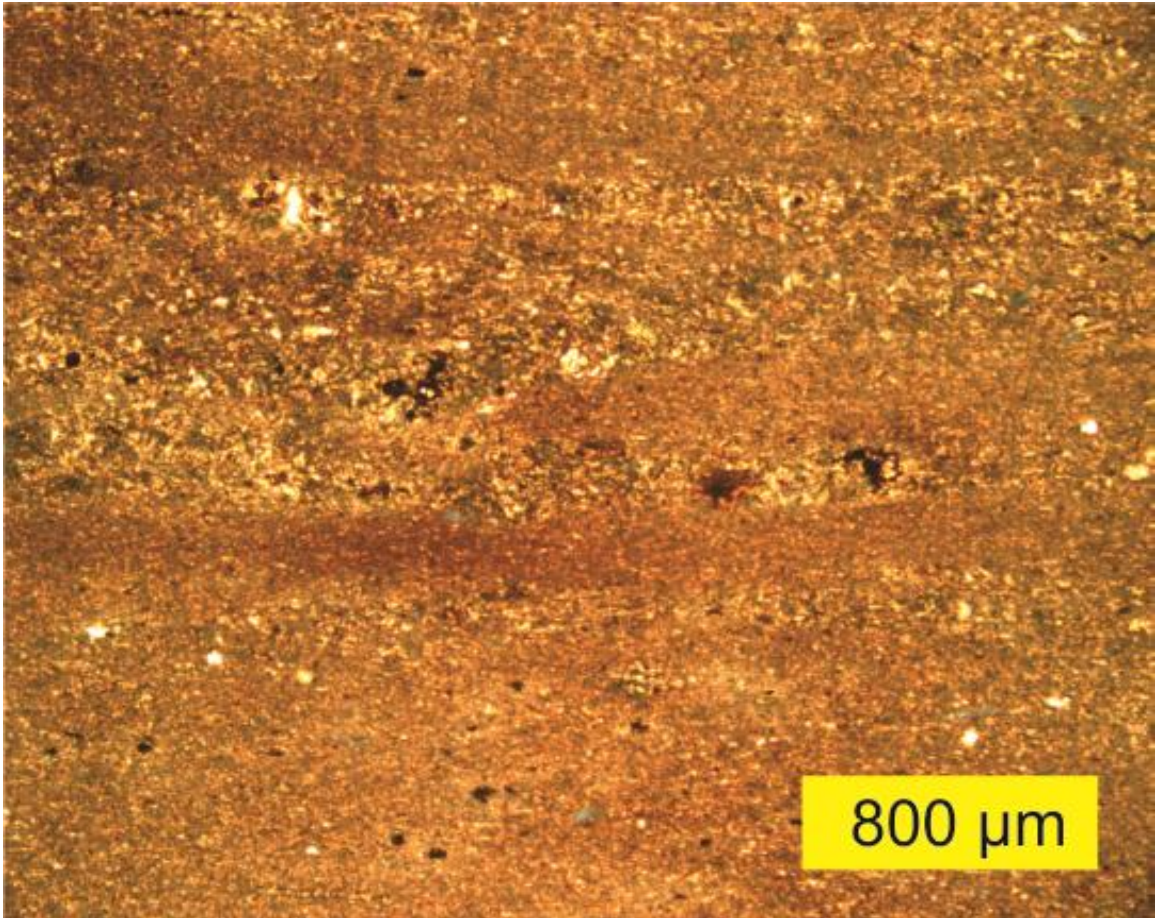
Sample ISP1-8



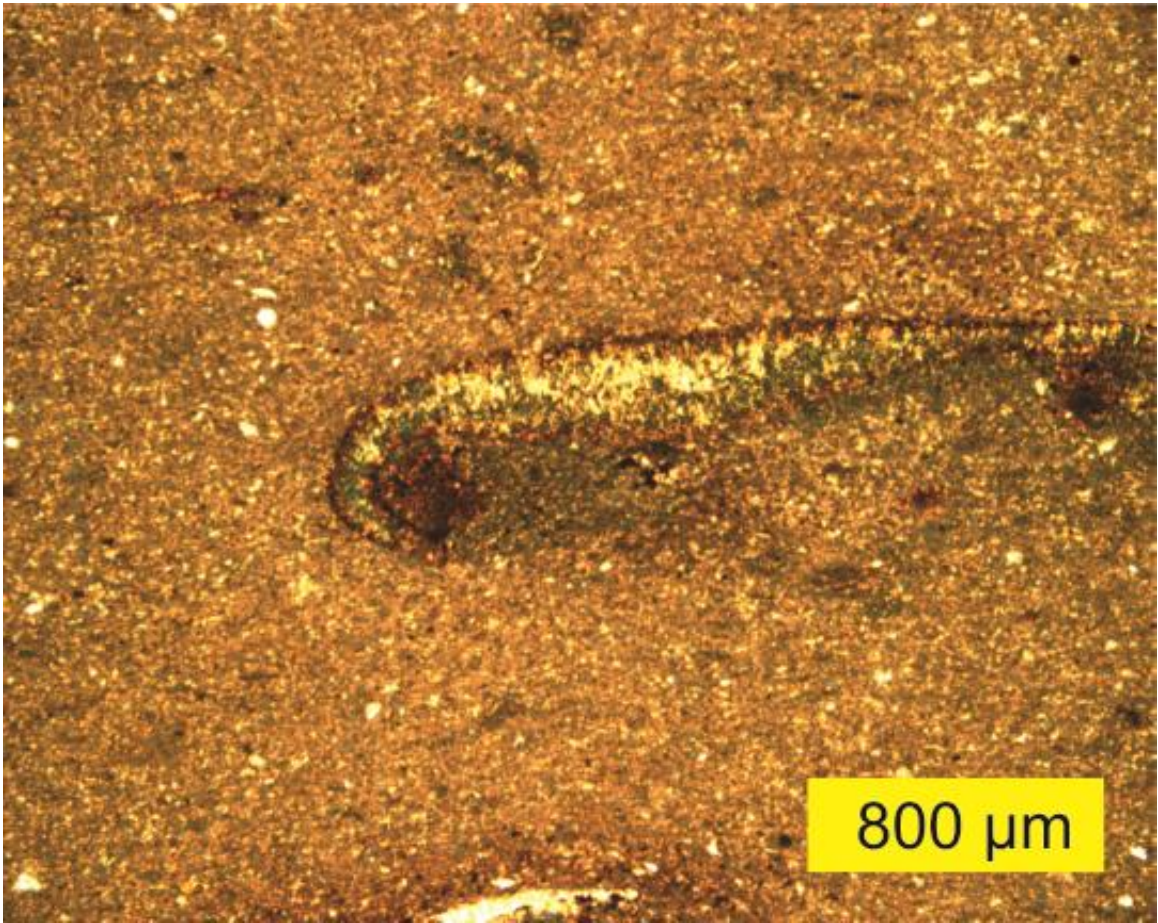
Sample ISP2-1



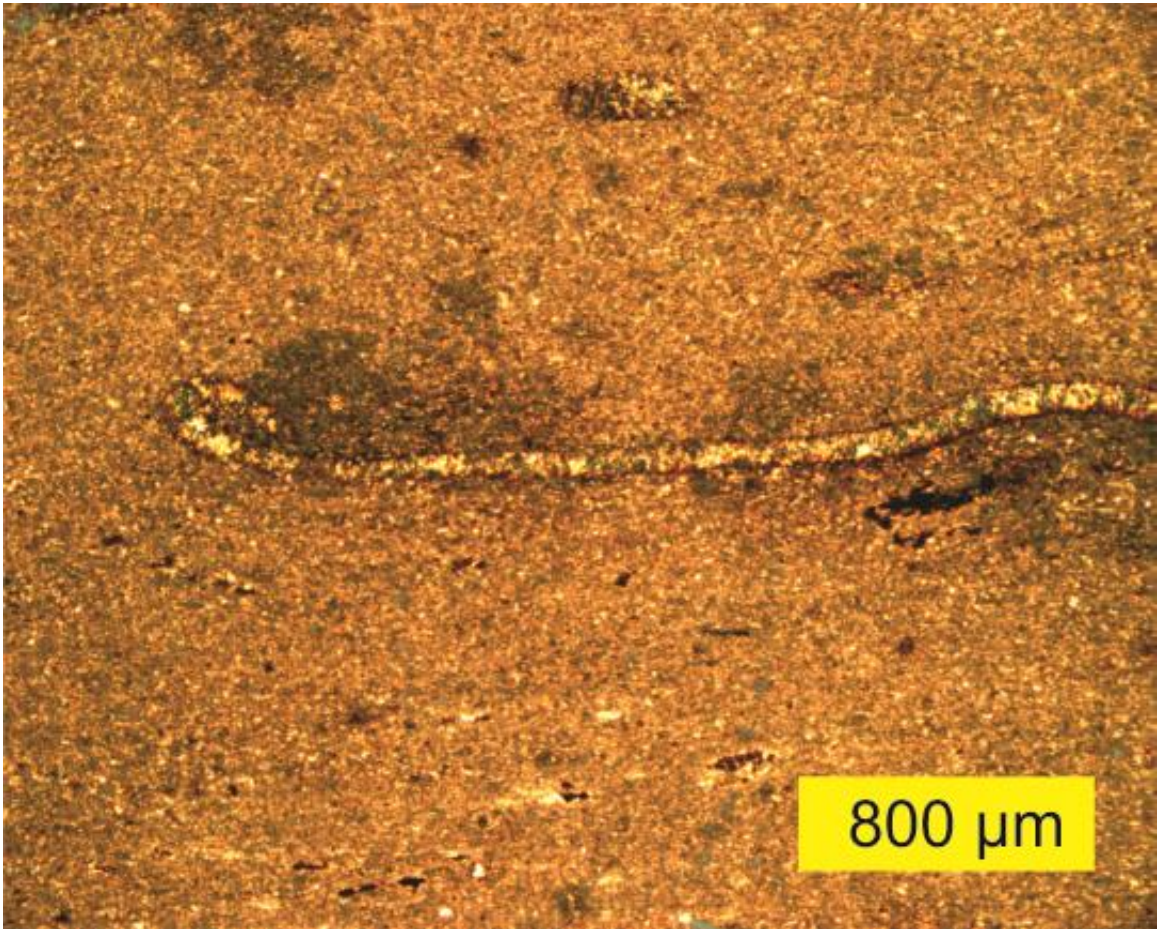
Sample ISP2-2



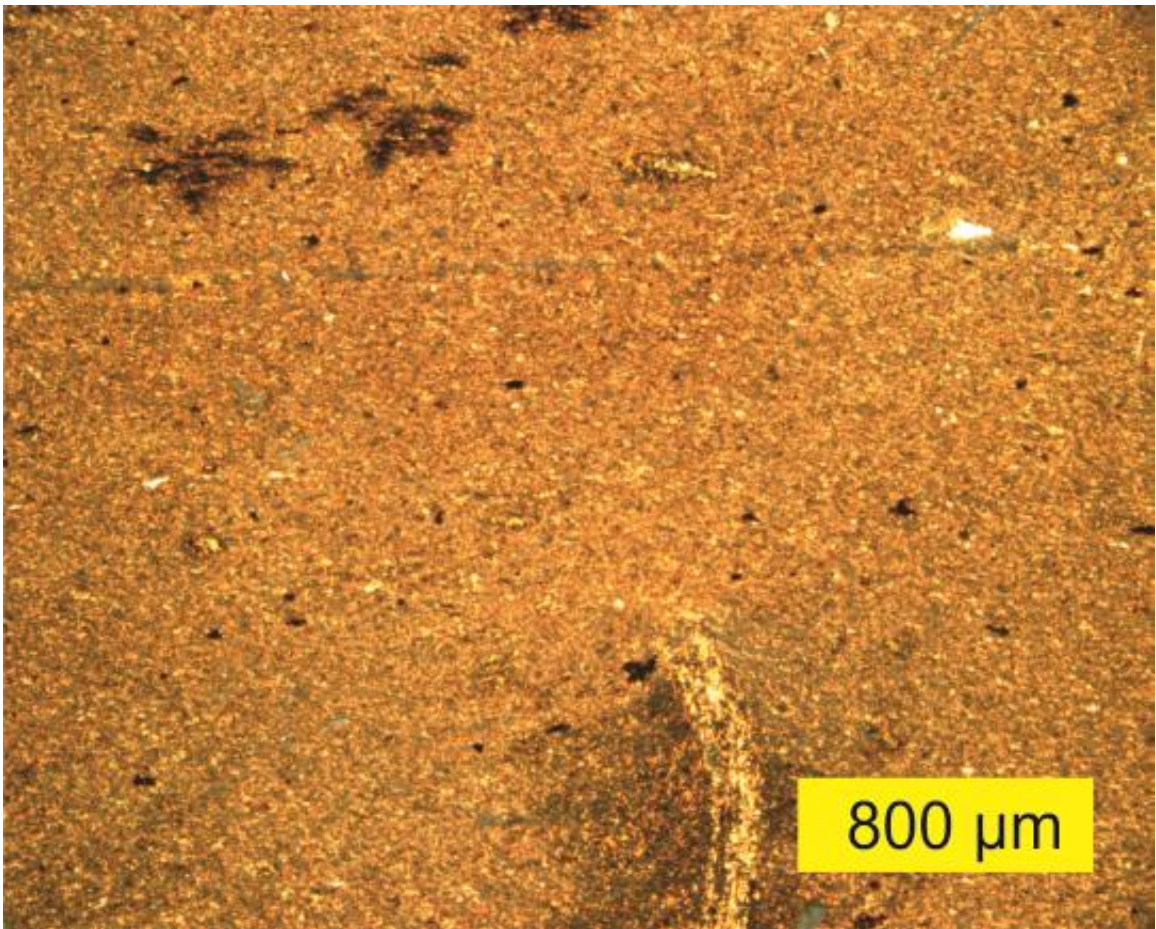
Sample ISP2-3



Sample ISP2-4



Sample ISP2-6



**Appendix E:**  
**XRF Geochemical Data**

XRF Results for 20 m section from the Indian Springs Canyon locality. Trace elemental compositions in PPM.

Formula	ISP1-1A	ISP1-1B	ISP1-2	ISP1-3	ISP1-4	ISP1-5	ISP1-6	ISP1-7	ISP1-8
Mn	0.02%	0.02%	0.02%	0.01%	0.02%	0.17%	0.01%	0.02%	0.02%
Na <sub>2</sub> O	0.12%	0.09%	0.12%	0.14%	0.11%	0.08%	0.13%	0.12%	0.14%
MgO	2.40%	2.54%	2.36%	2.31%	2.36%	2.82%	2.23%	2.58%	2.34%
Al <sub>2</sub> O <sub>3</sub>	20.28%	18.45%	19.98%	20.22%	20.08%	16.56%	19.54%	19.88%	19.84%
SiO <sub>2</sub>	56.78%	58.81%	56.76%	56.98%	56.48%	57.31%	58.45%	56.74%	56.84%
P <sub>2</sub> O <sub>5</sub>	0.12%	0.12%	0.11%	0.12%	0.12%	0.21%	0.12%	0.15%	0.16%
K <sub>2</sub> O	5.13%	4.37%	5.13%	5.14%	4.98%	3.25%	4.93%	4.81%	4.95%
CaO	0.38%	0.38%	0.37%	0.39%	0.43%	0.83%	0.38%	0.42%	0.48%
TiO <sub>2</sub>	0.83%	0.80%	0.80%	0.80%	0.80%	0.68%	0.80%	0.83%	0.80%
Fe <sub>2</sub> O <sub>3</sub>	7.69%	8.18%	7.71%	7.22%	7.63%	10.41%	7.28%	7.99%	7.80%
Y	35	36	38	38	38	38	35	35	37
Zr	149	162	138	152	147	149	149	154	139
Nb	26	21	29	34	27	26	25	25	29
V	105	94	103	105	112	92	104	84	103
Zn	109	110	106	107	110	117	96	111	93
Ni	57	53	57	53	49	54	55	55	55
Cr	104	93	102	117	117	71	89	115	98
Co	12	32	22	20	37	44	25	29	24
Ce	184	135	190	157	226	215	221	258	206
Sr	43	36	45	42	26	40	28	42	26
Ba	506	492	508	492	468	398	497	435	479
LOI	4.84	4.51	5.00	4.83	7.85	5.71	4.70	4.93	4.81
SUM	98.72%	98.41%	98.48%	98.38%	100.99%	98.14%	98.68%	98.59%	98.33%

XRF Results for 65 m section from the Indian Springs Canyon locality. Trace elemental compositions in PPM.

Formula	ISP2-1	ISP2-2	ISP2-3	ISP2-4	ISP2-5	ISP2-6	ISP2-7	ISP2-8	ISP2-9
Mn	0.18%	0.02%	0.02%	0.03%	0.05%	0.03%	0.03%	0.02%	0.02%
Na <sub>2</sub> O	0.10%	0.17%	0.15%	0.17%	0.17%	0.16%	0.15%	0.15%	0.15%
MgO	2.04%	2.27%	2.54%	2.57%	2.39%	2.53%	3.08%	2.56%	2.38%
Al <sub>2</sub> O <sub>3</sub>	10.99%	20.21%	19.19%	18.75%	19.22%	19.58%	19.62%	19.61%	19.20%
SiO <sub>2</sub>	31.43%	57.99%	57.40%	56.30%	57.75%	57.93%	56.68%	57.95%	58.44%
P <sub>2</sub> O <sub>5</sub>	0.15%	0.12%	0.13%	0.13%	0.12%	0.13%	0.13%	0.11%	0.13%
K <sub>2</sub> O	2.39%	5.01%	4.48%	4.27%	4.51%	4.55%	4.22%	4.57%	4.56%
CaO	24.97%	0.39%	0.92%	1.25%	0.78%	0.89%	0.39%	0.69%	0.90%
TiO <sub>2</sub>	0.44%	0.86%	0.83%	0.83%	0.83%	0.82%	0.83%	0.80%	0.82%
Fe <sub>2</sub> O <sub>3</sub>	5.99%	6.64%	7.68%	7.69%	7.39%	7.62%	9.26%	7.35%	6.86%
Y	30	36	35	35	35	35	33	37	35
Zr	84	165	164	170	158	156	150	151	156
Nb	21	27	25	31	26	28	25	28	27
V	65	106	98	100	86	119	107	100	103
Zn	97	98	111	106	121	116	144	115	104
Ni	29	51	55	60	49	53	67	62	57
Cr	86	98	101	107	83	106	160	96	108
Co	30	27	32	22	45	26	20	32	24
Ce	132	178	278	212	169	309	317	201	142
Sr	147	51	52	56	60	54	54	68	57
Ba	332	732	609	637	699	666	588	656	733
LOI	21.75	4.51	4.88	5.24	5.03	4.60	4.85	4.89	4.90
SUM	100.54%	98.35%	98.37%	97.37%	98.40%	97.76%	98.17%	98.85%	98.52%

XRF Results for 95 m section from the Indian Springs Canyon locality. Trace elemental compositions in PPM.

Formula	ISP3-1	ISP3-2	ISP3-3	ISP3-4	ISP3-5	ISP3-6
Mn	0.02%	0.03%	0.04%	0.07%	0.03%	0.03%
Na <sub>2</sub> O	2.49%	2.44%	2.14%	2.14%	2.18%	2.22%
MgO	0.64%	0.65%	0.53%	0.40%	0.45%	0.50%
Al <sub>2</sub> O <sub>3</sub>	6.65%	6.48%	5.58%	5.75%	5.98%	7.18%
SiO <sub>2</sub>	75.92%	78.13%	75.40%	69.53%	79.30%	82.76%
P <sub>2</sub> O <sub>5</sub>	0.04%	0.04%	0.04%	0.04%	0.04%	0.04%
K <sub>2</sub> O	0.33%	0.27%	0.21%	0.24%	0.25%	0.39%
CaO	2.91%	4.47%	7.19%	10.71%	4.69%	1.72%
TiO <sub>2</sub>	0.26%	0.23%	0.23%	0.22%	0.24%	0.25%
Fe <sub>2</sub> O <sub>3</sub>	1.69%	1.80%	1.49%	1.05%	1.29%	1.47%
Y	19	21	22	20	21	20
Zr	361	341	362	335	377	346
Nb	11	12	17	13	16	7
V	5	6	10	10	8	15
Zn	41	32	23	23	14	30
Ni	-2	13	10	-11	-3	6
Cr	28	30	16	29	31	49
Co	68	65	32	36	70	116
Ce	155	119	94	117	171	139
Sr	29	46	48	86	49	36
Ba	162	137	104	238	437	397
LOI	3.44	4.70	6.69	9.29	4.63	2.58
SUM	94.49%	99.31%	99.61%	99.52%	99.20%	99.26%

XRF Results for 105 m section from the Indian Springs Canyon locality. Trace elemental compositions in PPM.

<b>Formula</b>	<b>ISP4-1</b>	<b>ISP4-2</b>	<b>ISP4-3</b>	<b>ISP4-4</b>
Mn	0.23%	0.24%	0.15%	0.11%
Na <sub>2</sub> O	0.01%	0.02%	0.04%	0.04%
MgO	0.50%	0.33%	2.28%	1.01%
Al <sub>2</sub> O <sub>3</sub>	1.74%	2.33%	10.70%	8.22%
SiO <sub>2</sub>	6.80%	13.20%	29.26%	40.92%
P <sub>2</sub> O <sub>5</sub>	0.04%	0.04%	0.08%	0.08%
K <sub>2</sub> O	0.24%	0.14%	2.49%	0.61%
CaO	52.35%	52.42%	25.29%	23.07%
TiO <sub>2</sub>	0.06%	0.12%	0.43%	0.38%
Fe <sub>2</sub> O <sub>3</sub>	1.25%	1.17%	7.79%	5.21%
Y	18	20	30	27
Zr	12	84	94	266
Nb	8	8	23	15
V	9	9	49	26
Zn	18	7	103	60
Ni	-20	-12	22	17
Cr	15	26	65	29
Co	8	-2	19	23
Ce	125	102	161	153
Sr	217	176	122	67
Ba	17	63	241	82
LOI	39.51	36.72	22.40	20.44
SUM	102.77%	107.77%	101.01%	100.16%

XRF Results for 20 m quadrat section from the Indian Springs Canyon locality. Trace elemental compositions in PPM.

Formula	ISPQ1-1	ISPQ1-2	ISPQ1-3	ISPQ1-4	ISPQ1-5
Mn	0.02%	0.02%	0.04%	0.02%	0.02%
Na <sub>2</sub> O	0.12%	0.14%	0.10%	0.13%	0.12%
MgO	2.30%	2.25%	2.79%	2.56%	2.46%
Al <sub>2</sub> O <sub>3</sub>	20.21%	20.15%	19.27%	20.57%	19.91%
SiO <sub>2</sub>	56.44%	57.80%	58.08%	59.36%	58.93%
P <sub>2</sub> O <sub>5</sub>	0.12%	0.12%	0.13%	0.11%	0.12%
K <sub>2</sub> O	5.00%	5.15%	4.55%	5.05%	4.90%
CaO	0.45%	0.32%	0.34%	0.29%	0.35%
TiO <sub>2</sub>	0.80%	0.80%	0.79%	0.85%	0.79%
Fe <sub>2</sub> O <sub>3</sub>	7.84%	6.90%	8.12%	7.73%	7.45%
Y	35	38	35	39	40
Zr	146	147	160	152	150
Nb	27	28	23	35	28
V	107	100	89	99	91
Zn	109	92	105	91	84
Ni	52	48	55	58	48
Cr	115	102	101	102	91
Co	34	28	28	44	22
Ce	221	188	272	200	219
Sr	38	42	30	58	33
Ba	462	517	420	580	542
LOI	4.87	4.54	4.59	4.67	4.68
SUM	98.30%	98.33%	98.92%	101.49%	99.86%

XRF Results for 65 m quadrat section from the Indian Springs Canyon locality. Trace elemental compositions in PPM.

<b>Formula</b>	<b>ISPQ2-1</b>	<b>ISPQ2-2</b>	<b>ISPQ2-3</b>	<b>ISPQ2-4</b>	<b>ISPQ2-5</b>
Mn	0.03%	0.02%	0.02%	0.05%	0.02%
Na <sub>2</sub> O	0.18%	0.15%	0.15%	0.00%	0.17%
MgO	2.10%	2.23%	2.13%	0.47%	1.80%
Al <sub>2</sub> O <sub>3</sub>	20.64%	20.57%	19.73%	3.85%	19.94%
SiO <sub>2</sub>	60.02%	60.19%	60.30%	80.66%	59.72%
P <sub>2</sub> O <sub>5</sub>	0.12%	0.13%	0.12%	0.09%	0.11%
K <sub>2</sub> O	5.11%	4.88%	4.68%	0.42%	5.23%
CaO	0.32%	0.34%	0.41%	6.01%	0.22%
TiO <sub>2</sub>	0.86%	0.87%	0.84%	0.26%	0.84%
Fe <sub>2</sub> O <sub>3</sub>	7.23%	6.52%	6.77%	2.35%	7.14%
Y	36	39	36	23	44
Zr	162	163	163	409	413
Nb	31	33	29	10	68
V	102	98	107	9	98
Zn	76	95	96	12	77
Ni	46	50	54	2	46
Cr	102	115	108	6	87
Co	60	34	37	61	48
Ce	194	278	224	202	279
Sr	54	36	35	-17	43
Ba	718	569	574	64	793
LOI	4.40	0.93	4.33	6.06	4.11
SUM	101.16%	96.98%	99.62%	100.30%	99.50%

XRF Results for 95 m quadrat section from the Indian Springs Canyon locality. Trace elemental compositions in PPM.

Formula	ISPQ3-1	ISPQ3-2	ISPQ3-3	ISPQ3-4	ISPQ3-5
Mn	0.02%	0.30%	0.01%	0.13%	0.14%
Na <sub>2</sub> O	0.10%	0.15%	0.38%	0.03%	0.03%
MgO	2.40%	0.54%	0.96%	0.77%	1.15%
Al <sub>2</sub> O <sub>3</sub>	18.77%	1.31%	4.88%	6.18%	7.38%
SiO <sub>2</sub>	60.06%	7.91%	89.38%	26.62%	38.14%
P <sub>2</sub> O <sub>5</sub>	0.12%	0.05%	0.07%	0.07%	0.08%
K <sub>2</sub> O	5.12%	0.10%	0.43%	0.63%	0.74%
CaO	0.89%	58.47%	0.43%	37.04%	29.12%
TiO <sub>2</sub>	0.86%	0.06%	0.23%	0.34%	0.44%
Fe <sub>2</sub> O <sub>3</sub>	6.78%	1.16%	2.25%	2.68%	3.58%
Y	39	17	21	27	30
Zr	215	36	319	193	300
Nb	31	3	16	19	14
V	ND	ND	ND	ND	ND
Zn	102	26	26	21	51
Ni	ND	ND	ND	ND	ND
Cr	ND	ND	ND	ND	ND
Co	43	4	160	14	19
Ce	203	88	168	145	210
Sr	27	358	ND	324	128
Ba	566	128	56	14	54
LOI	5.20	38.59	2.11	29.14	4.80
SUM	100.46%	108.69%	101.22%	103.72%	85.69%

XRF Results for 105 m quadrat section from the Indian Springs Canyon locality. Trace elemental compositions in PPM.

Formula	ISPQ4-1	ISPQ4-2	ISPQ4-3	ISPQ4-4	ISPQ4-5
Mn	0.03%	0.11%	0.05%	0.12%	0.01%
Na <sub>2</sub> O	0.60%	0.02%	0.03%	0.03%	0.02%
MgO	2.02%	0.51%	0.97%	1.27%	0.22%
Al <sub>2</sub> O <sub>3</sub>	8.45%	5.70%	8.14%	8.06%	5.81%
SiO <sub>2</sub>	71.37%	32.98%	56.56%	39.56%	90.32%
P <sub>2</sub> O <sub>5</sub>	0.12%	0.09%	0.11%	0.10%	0.06%
K <sub>2</sub> O	0.92%	0.36%	0.89%	1.14%	0.63%
CaO	2.49%	33.71%	16.14%	24.52%	0.15%
TiO <sub>2</sub>	0.52%	0.27%	0.40%	0.40%	0.31%
Fe <sub>2</sub> O <sub>3</sub>	5.60%	2.08%	1.99%	4.78%	0.42%
Y	34	26	23	26	21
Zr	829	185	314	251	484
Nb	18	14	19	16	21
V	ND	ND	ND	ND	ND
Zn	97	19	45	62	5
Ni	ND	ND	ND	ND	ND
Cr	23	31	66	47	46
Co	83	4	24	27	154
Ce	199	184	198	188	160
Sr	46	145	11	108	-12
Ba	192	ND	77	74	16
LOI	23.35	26.92	15.06	21.35	1.85
SUM	115.63%	102.81	100.42%	101.41%	99.89%

XRF Results for Westgard Pass, White-Inyo Mountains locality. Trace elemental compositions in PPM.

Formula	D1	D2	D3	D5	D6	D7	D8	D11	D12
Mn	0.02%	0.02%	0.03%	0.02%	0.03%	0.05%	0.16%	0.04%	0.26%
Na <sub>2</sub> O	1.35%	1.24%	1.22%	1.08%	1.18%	1.00%	2.17%	1.33%	1.42%
MgO	2.09%	2.20%	2.36%	1.98%	2.75%	2.57%	1.90%	2.48%	1.35%
Al <sub>2</sub> O <sub>3</sub>	18.74%	19.16%	18.58%	20.55%	19.00%	19.62%	9.64%	17.31%	4.85%
SiO <sub>2</sub>	59.93%	59.84%	60.17%	58.44%	57.09%	56.78%	47.28%	59.19%	27.19%
P <sub>2</sub> O <sub>5</sub>	0.14%	0.13%	0.13%	0.13%	0.14%	0.14%	0.14%	0.13%	0.11%
K <sub>2</sub> O	4.29%	4.36%	4.17%	5.08%	4.13%	4.48%	1.01%	3.63%	0.20%
CaO	0.94%	0.24%	0.50%	0.23%	0.96%	1.11%	16.39%	1.48%	35.29%
TiO <sub>2</sub>	0.88%	0.83%	0.83%	0.89%	0.84%	0.84%	0.55%	0.82%	0.29%
Fe <sub>2</sub> O <sub>3</sub>	6.06%	5.99%	6.73%	5.87%	7.80%	7.32%	5.27%	7.08%	3.59%
Y	35	31	33	34	36	35	27	32	25
Zr	219	180	189	170	182	161	245	187	146
Nb	30	29	29	31	27	30	19	29	9
V	108	81	98	108	101	109	50	84	ND
Zn	90	96	105	88	108	93	73	115	63
Ni	41	42	51	34	51	41	20	49	ND
Cr	99	98	90	111	101	102	65	90	ND
Co	22	18	20	26	34	39	14	32	8
Ce	163	198	187	200	183	247	197	185	111
Sr	148	139	128	145	154	156	510	156	806
Ba	622	590	571	706	561	601	112	543	ND
LOI	4.54	12.86	4.24	4.24	4.53	4.95	14.60	4.58	27.38
SUM	99.13%	107.01%	99.10%	98.66%	98.62%	99.02%	99.25%	98.22%	102.06%

Paleoredox indices calculations (V/Cr and V/(V+Ni)) from the 20 m section from the Indian Springs Canyon locality.

Redox-sensitive elements V, Cr, and Ni abundances in PPM.

<b>Sample</b>	<b>V</b>	<b>Cr</b>	<b>Ni</b>	<b>V/Cr</b>	<b>V/(V+Ni)</b>
ISP1-1A	105	104	57	1.01	0.65
ISP1-1B	94	93	53	1.01	0.64
ISP1-2	103	102	57	1.01	0.64
ISP1-3	105	117	53	0.90	0.66
ISP1-4	112	117	49	0.95	0.70
ISP1-5	92	71	54	1.30	0.63
ISP1-6	104	89	55	1.16	0.66
ISP1-7	84	115	55	0.73	0.60
ISP1-8	103	98	55	1.05	0.65

Paleoredox indices calculations (V/Cr and V/(V+Ni)) from the 65 m section from the Indian Springs Canyon locality.

Redox-sensitive elements V, Cr, and Ni abundances in PPM.

<b>Sample</b>	<b>V</b>	<b>Cr</b>	<b>Ni</b>	<b>V/Cr</b>	<b>V/(V+Ni)</b>
ISP2-1	65	86	29	0.76	0.69
ISP2-2	106	98	51	1.08	0.68
ISP2-3	98	101	55	0.98	0.64
ISP2-4	100	107	60	0.94	0.63
ISP2-5	86	83	49	1.04	0.64
ISP2-6	119	106	53	1.12	0.69
ISP2-7	107	160	67	0.67	0.62
ISP2-8	100	96	62	1.04	0.62
ISP2-9	103	108	57	0.96	0.65

Paleoredox indices calculations ( $V/Cr$  and  $V/(V+Ni)$ ) from the 95 m section (Samples ISP3-1 through ISP3-6) from the Indian Springs Canyon locality yielded non-detectable abundances.

Paleoredox indices calculations ( $V/Cr$  and  $V/(V+Ni)$ ) from the 105 m section (Samples ISP4-1 through ISP4-4) from the Indian Springs Canyon locality yielded non-detectable abundances.

Paleoredox indices calculations (V/Cr and V/(V+Ni)) from the 20 m quadrat section from the Indian Springs Canyon locality.

Redox-sensitive elements V, Cr, and Ni abundances in PPM.

<b>Sample</b>	<b>V</b>	<b>Cr</b>	<b>Ni</b>	<b>V/Cr</b>	<b>V/(V+Ni)</b>
ISPQ1-1	107	115	52	0.93	0.67
ISPQ1-2	100	102	48	0.98	0.67
ISPQ1-3	89	101	55	0.88	0.62
ISPQ1-4	99	102	58	0.97	0.63
ISPQ1-5	91	91	48	1.00	0.66

Paleoredox indices calculations (V/Cr and V/(V+Ni)) from the 65 m quadrat section from the Indian Springs Canyon locality.

Redox-sensitive elements V, Cr, and Ni abundances in PPM.

<b>Sample</b>	<b>V</b>	<b>Cr</b>	<b>Ni</b>	<b>V/Cr</b>	<b>V/(V+Ni)</b>
ISPQ2-1	102	102	46	1.00	0.69
ISPQ2-2	98	115	50	0.85	0.66
ISPQ2-3	107	108	54	0.99	0.66
ISPQ2-4	ND	ND	ND	ND	ND
ISPQ2-5	98	87	46	1.14	0.68

Paleoredox indices calculations (V/Cr and V/(V+Ni)) from the 95 m quadrat section from the Indian Springs Canyon locality.

Redox-sensitive elements V, Cr, and Ni abundances in PPM.

<b>Sample</b>	<b>V</b>	<b>Cr</b>	<b>Ni</b>	<b>V/Cr</b>	<b>V/(V+Ni)</b>
ISPQ3-1	77	98	47	0.79	0.62
ISPQ3-2	ND	22	ND	ND	ND
ISPQ3-3	ND	30	ND	ND	ND
ISPQ3-4	19	29	ND	0.63	ND
ISPQ3-5	25	45	ND	0.54	ND

Paleoredox indices calculations (V/Cr and V/(V+Ni)) from the 105 m quadrat section from the Indian Springs Canyon locality.

Redox-sensitive elements V, Cr, and Ni abundances in PPM.

<b>Sample</b>	<b>V</b>	<b>Cr</b>	<b>Ni</b>	<b>V/Cr</b>	<b>V/(V+Ni)</b>
ISPQ4-1	19	23	40	0.80	0.32
ISPQ4-2	ND	ND	ND	ND	ND
ISPQ4-3	19	66	20	0.28	0.49
ISPQ4-4	ND	47	ND	ND	ND
ISPQ4-5	ND	46	ND	ND	ND

Paleoredox indices calculations (V/Cr and V/(V+Ni)) from the Westgard Pass, White-Inyo Mountains locality.

Redox-sensitive elements V, Cr, and Ni abundances in PPM.

<b>Sample</b>	<b>V</b>	<b>Cr</b>	<b>Ni</b>	<b>V/Cr</b>	<b>V/(V+Ni)</b>
D1	108	99	41	1.09	0.72
D2	81	98	42	0.83	0.66
D3	98	90	51	1.09	0.66
D5	108	111	34	0.97	0.76
D6	101	101	51	0.99	0.66
D7	109	102	41	1.07	0.73
D8	50	65	20	0.77	0.72
D11	84	90	49	0.93	0.63
D12	ND	ND	ND	ND	ND

**Appendix F:**  
**Ichnofabric Index Data and Measurements**

## Ichnofabric Index data (mm-scale) for the 20 m section (ISP1) at the Indian Springs

Canyon locality.

<b>Sample</b>	<b>Total count (mm)</b>	<b>ii1</b>	<b>ii2</b>	<b>ii3</b>	<b>ii4</b>	<b>ii5</b>
ISP1-1A	26	26	0	0	0	0
ISP1-1B	43	43	0	0	0	0
ISP1-2	40	40	0	0	0	0
ISP1-3	40	40	0	0	0	0
ISP1-4	35	22	13	0	0	0
ISP1-5	30	15	15	0	0	0
ISP1-6	47	26	21	0	0	0
ISP1-7	40	28	12	0	0	0
ISP1-8	44	30	14	0	0	0
Subtotal	345	270	75	0	0	0

Average ii: 1.21

Ichnofabric Index data (mm-scale) for the 265 m section (ISP2) at the Indian Springs

Canyon locality.

<b>Sample</b>	<b>Total count (mm)</b>	<b>ii1</b>	<b>ii2</b>	<b>ii3</b>	<b>ii4</b>	<b>ii5</b>
ISP2-1	30	30	0	0	0	0
ISP2-2	35	35	0	0	0	0
ISP2-3	13	13	0	0	0	0
ISP2-4	45	20	25	0	0	0
ISP2-5	19	5	5	9	0	0
ISP2-6	23	9	8	6	0	0
ISP2-7	15	3	12	0	0	0
ISP2-8	15	15	0	0	0	0
ISP2-9	14	14	0	0	0	0
Subtotal	209	144	50	15	0	0

Average ii: 1.38